



On the Thermodynamic and Dynamic Aspects of Immersion Ice Nucleation

Donifan Barahona¹

¹NASA Goddard Space Flight Center, Greenbelt, MD, USA

Correspondence to: Donifan Barahona (donifan.o.barahona@nasa.gov)

Abstract.

Heterogeneous ice nucleation initiated by particles immersed within droplets is likely the main pathway of ice formation in the atmosphere. Theoretical models commonly used to describe this process assume that it mimics ice formation from the vapor, neglecting interactions unique to the liquid phase. This work introduces a new approach that accounts for such interactions by linking the ability of particles to promote ice formation to the modification of the properties of water near the particle-liquid interface. It is shown that the same mechanism that lowers the thermodynamic barrier for ice nucleation also tends to decrease the mobility of water molecules, hence the ice-liquid interfacial flux. Heterogeneous ice nucleation in the liquid phase is thus determined by the competition between thermodynamic and kinetic constraints to the formation and propagation of ice. At the limit, ice nucleation may be mediated by the dynamics of vicinal water instead of the nucleation work. This new ice nucleation regime is termed spinodal ice nucleation. Comparison of predicted nucleation rates against published data suggests that some materials of atmospheric relevance may nucleate ice in this regime.

1 Introduction

Ice nucleation in cloud droplets and aerosol particles leads to cloud formation and glaciation at low temperature. It is often initiated by certain aerosol species known as ice nucleating particles (INP) (DeMott et al., 2003; Cziczo et al., 2013; Barahona et al., 2017). These include dust, biological particles, metals, effloresced sulfate and sea salt, organic material and soot (Murray et al., 2012; Hoose and Möhler, 2012). Background INP concentrations may be influenced by aerosol emissions (Lohmann and Feichter, 2005). Anthropogenic activities may thus alter the formation and evolution of ice clouds leading to an indirect effect on climate. The assessment of the role of INP on climate is challenging due to the complexity of the atmospheric processes involving ice and the limited understanding of the ice nucleation mechanism of INP (Myhre et al., 2013). Ice nucleation promoted by a particle completely immersed within the liquid phase, referred as “immersion freezing”, is likely the most common ice formation pathway in the atmosphere (DeMott et al., 2003; Wiacek et al., 2010). Immersion freezing is involved in the initiation of precipitation and determines to a large extent the phase partitioning in convective clouds (Diehl and Wurzler, 2004; Wiacek et al., 2010; Lance et al., 2011; Murray et al., 2012).

The accurate representation of immersion ice nucleation is critical for the correct modeling of cloud processes in atmospheric models (Hoose and Möhler, 2012; Murray et al., 2012; Tan et al., 2016). Field campaign data have been used to develop empir-



ical formulations relating the INP concentration to the cloud temperature, T , and saturation ratio, S_i (e.g., Bigg, 1953; Fletcher, 1959; Meyers et al., 1992), and more recently to the ambient aerosol size and composition (e.g., DeMott et al., 2010; Niemand et al., 2012; Phillips et al., 2013). Empirical formulations provide a simple way to parameterize ice nucleation in atmospheric models (e.g., Gettelman et al., 2012; Barahona et al., 2014). However they may not be valid outside the conditions used in their
5 development, particularly as different experimental techniques may result on a wide range of measured ice nucleation efficiencies (Hiranuma et al., 2015). Alternatively, the ice nucleation efficiency can be empirically parameterized using laboratory data, although with similar caveats (Knopf and Alpert, 2013; Murray et al., 2012).

Molecular dynamics (MD) simulations and direct kinetic methods have been used to study ice nucleation (e.g., Taylor and Hale, 1993; Matsumoto et al., 2002; Lupi et al., 2014; Espinosa et al., 2014). However, the classical nucleation theory (CNT) is
10 nearly the only theoretical approach employed to describe immersion freezing in cloud models (e.g., Khvorostyanov and Curry, 2004a; Barahona and Nenes, 2008, 2009; Hoose et al., 2010). According to CNT, nucleation is initiated by a cap-shaped ice germ on the surface of the immersed particle which grows by random collision of water molecules (Pruppacher and Klett, 1997; Kashchiev, 2000). The geometry of the ice germ is defined by a force balance at the particle-ice-liquid interface, described by the contact angle, θ . In this sense, the ice germ is assumed to “wet” the immersed particle in the same way a liquid droplet wets
15 a solid surface (De Gennes, 1985). Low values of θ indicate a high affinity of the particle for ice and a low energy of formation of the ice germ.

Direct application of CNT in immersion freezing is thwarted by uncertainty in fundamental parameters of the theory as for example the ice-liquid interfacial energy, σ_{iw} , and the activation energy. Moreover, using a single θ to describe the nucleation efficiency of dust and other materials typically leads to large discrepancy between CNT predictions and experimental mea-
20 surements (e.g., Zobrist et al., 2007; Alpert et al., 2011; Broadley et al., 2012; Rigg et al., 2013). More fundamentally, CNT neglects important interactions near the immersed particle that may influence the nucleation rate. MD simulations show that an ice germ formed near a surface tends to have a complex geometry instead cap-shaped assumption of CNT (e.g. Lupi et al., 2014; Cox et al., 2015; Fitzner et al., 2015). Also, in a liquid the ice germ would not “wet” the particle but rather exert stress on the substrate (Cahn, 1980; Rusanov, 2005). It is not clear that such force balance can be expressed in terms of a contact
25 angle (Cahn, 1980). It has been shown that σ_{iw} obtained by fitting CNT to measured nucleation rates tends to be biased high to account for mixing effects neglected in common formulations of the theory (Barahona, 2014).

Another fundamental assumption used in CNT is that ice nucleation solely depends on the local geometry of the absorbed molecules on the immersed particle (Kashchiev, 2000). This implies that the particle influences the formation of the ice germ but does not influence the adjacent water. The viscosity and density of water in the vicinity of the particle and in contact with
30 the ice germ are assumed similar to those in the bulk (Kashchiev, 2000). This is at odds with evidence of a strong effect of immersed particles on the vicinal water (Drost-Hansen, 1969; Michot et al., 2002). In fact, such an effect may be responsible for the enhancement of ice nucleation near immersed solids (Anderson, 1967).

To analyze how these interactions may affect immersion ice nucleation this work introduces a new approach to link the enhancement of the ice nucleation efficiency by immersed particles to the properties of vicinal water.



2 Theoretical development

2.1 Evidence for the formation of ordered structures near the liquid-particle interface

There is considerable evidence of the modification of the properties of vicinal water (i.e., the water immediately adjacent to the particle) by immersed surfaces. It has been known for some time that water near interfaces displays physicochemical properties different from those of the bulk (e.g., Drost-Hansen, 1969; Michot et al., 2002; Bellissent-Funel, 2002). By examining a wealth of available observations Drost-Hansen (1969) concluded that vicinal water may exist in an ordered state near the solid-liquid interface and that such ordered structures may propagate over considerable distance, of the order of hundreds to thousands of molecular diameters. More recent experiments showing that hydrophilic surfaces have a long-range impact further support this conclusion (e.g., Zheng et al., 2006). The interaction between the particle and the vicinal water becomes more significant as the temperature decreases and the viscosity increases (Wolfe et al., 2002). Recent studies have shown the presence of ordered water near interfaces in biological (Cooke and Kuntz, 1974; Snyder et al., 2014), metallic (Michot et al., 2002) and clay (Yu et al., 2001; Rinnert et al., 2005) particles, a notion that is also supported by molecular dynamics simulations (Lupi et al., 2014; Cox et al., 2015). In a groundbreaking work, Anderson (1967) found strong evidence of ice formation several molecular diameters away from the clay-water interface. The author concluded that ice formation does not require an ice germ attached to the substrate, but rather the nascent ice germ is stabilized by ordering in the interfacial zone. To date no quantitative theory has been developed exploiting such a view of ice nucleation.

The description of the properties of vicinal water is still under investigation. Early studies concluded that ordered water near immersed surfaces does not resemble a caltrate-like orientation of water molecules (Drost-Hansen, 1969). Rather, in the supercooled region the presence of structured low-density regions near solid surfaces (termed “ice-like”) has been reported for different materials (e.g., Etzler, 1983; Yu et al., 2001; Michaelides and Morgenstern, 2007; Feibelman, 2010; Snyder et al., 2014). In this region Etzler (1983) parameterized the density and enthalpy of vicinal water as an ideal mixture of ice-like and bulk-like water. Additional experimental observations show the modification of the mobility of vicinal water near interfaces; i.e., the vicinal water typically has a higher viscosity when compared to the bulk (Warne et al., 2000; Yu et al., 2001; Wolfe et al., 2002; Wang et al., 2006). In some cases, clays and biological systems exhibit a viscous layer of water at the particle-liquid interface that remains liquid even if the bulk has already frozen (Drost-Hansen, 1969). These effects are typically characterized as non-equilibrium, since they affect the flux of molecules to the nascent ice germ rather than the thermodynamics of ice nucleation. Li et al. (2014) found experimentally that the viscosity of interfacial water regulates the ice nucleation activity, giving support to the idea that the work of nucleation and the enhancement of the viscosity of the vicinal water are tightly linked. In fact, increased viscosity may be a necessary condition for ice nucleation since structural ordering is not possible in a fluid with low viscosity (Anderson, 1967).

These considerations are largely missing in the theoretical description of ice nucleation. There is currently no theory that can account for the thermodynamic and dynamic effects of an immersed particle on the surrounding water, hence on ice nucleation. To this end, an approach to describe the thermodynamics of vicinal water is introduced in Section 2.3. Then in Sections 2.3.1 and 2.4, it is used to develop quantitative models for the thermodynamics and dynamics of ice nucleation.



2.2 Classical Nucleation Theory

Since CNT is the most common theoretical approach used in atmospheric models we start by highlighting its main characteristics. Common CNT expressions use several assumptions to simplify the description of the interaction between water and the immersed particle (e.g., Khvorostyanov and Curry, 2004a; Zobrist et al., 2007; Hoose et al., 2010). Typically the energy of activation of water molecules near the particle is assumed to have the same value as in the bulk (Ickes et al., 2015). Other assumptions include a hemi-spherical ice germ, negligible surface stress (Cahn, 1980), and negligible mixing and dissipation effects during the germ formation (Barahona et al., 2014). These considerations lead to the commonly used expression for J_{het} (Turnbull and Fisher, 1949),

$$J_{\text{het, CNT}} = \frac{k_B T Z}{a_0 h} \exp \left[-\frac{\Delta G_{\text{act}} + g(\theta) \Delta G_{\text{hom, CNT}}}{k_B T} \right], \quad (1)$$

where ΔG_{act} is the activation energy, i.e., the energy required for a water molecule to leave its equilibrium position in the bulk towards the vicinity of the ice germ (Pruppacher and Klett, 1997; Zobrist et al., 2007) and h is Plank's constant. ΔG_{act} is assumed the same as in bulk water, hence it represents a barrier to "bulk" diffusion instead of interfacial transfer. Under this assumption structural transformations required to incorporate water molecules to the ice germ are also neglected. In general, ΔG_{act} is neither affected by the presence of the immersed particle nor the ice germ.

$\Delta G_{\text{hom, CNT}}$ is the homogeneous nucleation work, given by

$$\Delta G_{\text{hom, CNT}} = \frac{16\pi\sigma_{\text{iw}}^3 v_w^2}{3(k_B T \ln S_i)^2}, \quad (2)$$

where σ_{iw} is the ice-water interfacial energy. Typically σ_{iw} is empirically fitted to match measured nucleation rates. The effect of the immersed particle on $J_{\text{het, CNT}}$ depends on the adsorption of water molecules on individual sites, and it is characterized by the contact angle, θ in the form,

$$g(\theta) = \frac{1}{4}(2 + \cos\theta)(1 - \cos\theta)^2. \quad (3)$$

Equation (3) can be extended to account for line tension, curvature and misfit effects (e.g., Khvorostyanov and Curry, 2004a). Those are however neglected in this study.

It is clear that the CNT framework does not provide a way to link the properties of the vicinal water to the liquid-ice interfacial diffusion rate and the nucleation work, hence the nucleation rate. Accounting for such effects therefore requires a different approach, introduced in the next sections.



2.3 Thermodynamics of ice formation near the liquid-particle interface

The discussion presented in Section 2.1 suggests that the immersed particle enhances order near the particle-liquid interface, lowering the energy required to nucleate ice. Hence the first step towards linking immersion freezing to the properties of vicinal water is to develop a thermodynamic description of the latter.

5 The vicinal water differs from the bulk in that it contains a larger fraction of four-bonded, low density regions. Therefore it can be represented as a solution of ice-like and liquid-like “species”. In reality it is likely that vicinal water, just as bulk water, is made of a complex mixture of different water configurations (Reinhardt et al., 2012; Stanley and Teixeira, 1980). However two-state models have shown success in parameterizing the properties of supercooled water and are favored for their simplicity (Etzler, 1983; Holten et al., 2013). Within this framework it is assumed that Ice-Like (IL) and Liquid-Like
10 (LL) species with chemical potentials μ_{IL} and μ_{LL} , respectively, are mixed from their pure state forming a solution. During mixing some of the thermodynamic configurations available to each substance are lost due to the presence of the other solute, resulting in the entropy of mixing, ΔS_{mix} . The enthalpy and total entropy of each substance in solution may differ from their corresponding values in the pure state, leading to an excess free energy, g^E . If we denote by ζ the fraction of IL regions, then adding these contributions results in a equation of state for the vicinal water in the form,

$$15 \quad \mu_{\text{vc}} = (1 - \zeta)\mu_{\text{LL}} + \zeta\mu_{\text{IL}} + T\Delta S_{\text{mix}} + g^E, \quad (4)$$

The parameter ζ describes how efficiently the immersed particle enhances the ice-like behavior on the adjacent water, hence it acts as a “templating” factor. The limiting values $\zeta = 0$ and $\zeta = 1$ imply that vicinal water behaves as liquid-like or ice-like, respectively. Note that even for $\zeta = 0$ vicinal water likely has some IL configurations (which is the case for bulk supercooled water) and Eq. (4) merely represents a relative increase in the ice-like character near the immersed particle rather than absolute
20 fraction of low density regions.

Equation (4) can be reorganized in the the form,

$$\mu_{\text{vc}} = \mu_{\text{LL}} + \zeta(\mu_{\text{IL}} - \mu_{\text{LL}}) + T\Delta S_{\text{mix}} + g^E. \quad (5)$$

To express μ_{vc} in terms of measurable properties, two approximations are introduced. First ΔS_{mix} is given by the ideal entropy of mixing modified by a clustering factor, N , i.e.,

$$25 \quad \Delta S_{\text{mix}} = \frac{k_{\text{B}}}{N} [\zeta \ln(\zeta) + (1 - \zeta) \ln(1 - \zeta)]. \quad (6)$$

This approximation results from assuming random mixing and a weak interaction between IL and LL regions, which tend to cluster in groups of N molecules. Deviations from this behavior are in principle corrected by the excess energy, g^E , provided



a suitable expression is available. Since g^E must be negligible for $\zeta = 0$ and $\zeta = 1$ the simplest model describing this behavior takes the form,

$$g^E = -A_w \zeta(1 - \zeta), \quad (7)$$

where A_w is a phenomenological interaction parameter, and the negative sign accounts for the tendency of IL and LL regions to cluster (Tester et al., 1997). Using Eq. (6) and Eq. (7) within Eq. (5) and rearranging we obtain,

$$\mu_{vc} = \mu_{LL} + \zeta(\mu_{IL} - \mu_{LL}) + \frac{k_B T}{N} [\zeta \ln(\zeta) + (1 - \zeta) \ln(1 - \zeta)] - A_w \zeta(1 - \zeta), \quad (8)$$

This expression corresponds to a regular solution approximation to the properties of vicinal water. It has been previously used with success in describing the chemical potential of supercooled water (Holten et al., 2013). To use Eq. (8), it must be casted in terms of measurable variables. For this we notice that μ_{vc} has a critical temperature, T_c , at $\zeta = 0.5$, defined by the conditions (Holten et al., 2013),

$$\frac{\partial^2 \mu_{vc}}{\partial \zeta^2} = 0, \quad \frac{\partial^3 \mu_{vc}}{\partial \zeta^3} = 0. \quad (9)$$

Using Eq. (8) into Eq. (9) and solving for A_w gives for $T = T_c$,

$$A_w = \frac{2k_B T_c}{N}. \quad (10)$$

Physically, T_c represents the stability limit of the vicinal water, at which it spontaneously separates into IL and LL regions. To further simplify Eq. (8) we introduce the approximation,

$$\zeta(\mu_{IL} - \mu_{LL}) + T \Delta S_{\text{mix}} \approx \zeta \Delta \mu_s, \quad (11)$$

where $\Delta \mu_s$ is the free energy of solidification of water. Equation (11) is obtained by taking into account that the difference $\mu_{IL} - \mu_{LL}$, plus the energy of mixing, must approximate the energy released during freezing, hence its must be of the order of $\Delta \mu_s$. In reality $\Delta \mu_s$ corresponds to actual liquid and ice instead of the hypothetical LL and IL substances. Thus A_w plays the role of a semi-empirical correction factor accounting for, (i) the non-ideality originated from the mixing between the IL and the LL regions, and, (ii) the deviation of their chemical potentials from bulk ice and water, respectively.

Introducing Eqs. (7), (10) and (11), into Eq. (5) gives,

$$\mu_{vc} = \mu_{LL} + \zeta \Delta \mu_s - \frac{2k_B T_c}{N} \zeta(1 - \zeta). \quad (12)$$



Equation (12) is the expression sought. It describes the properties of vicinal water in terms of the material-specific parameter ζ , and the interaction parameters N and T_c . MD simulations indicate that $N \sim 6$ (Bullock and Molinero, 2013; Holten et al., 2013). T_c is thus the only remaining unknown in Eq. (12) and it is calculated at the point where the work of nucleation becomes negligible, as detailed in Section 2.3.3.

5 2.3.1 Work of germ formation

In immersion freezing the particle remains within the droplet long enough that equilibrium is established. This condition is mathematically expressed by the equality, $\mu_{vc} = \mu_w$, where μ_w is the chemical potential of water in the bulk of the liquid, i.e., away from the particle. Using Eq. (12) this implies,

$$\mu_w = \mu_{LL} + \zeta \Delta\mu_s - \frac{2k_B T_c}{N} \zeta (1 - \zeta). \quad (13)$$

- 10 This expression indicates that the effect of the particle on its vicinal water can be understood as an enhancement of the chemical potential of the LL regions, a consequence of the tendency of the particle to lower μ_{vc} . Since $\Delta\mu_s < 0$, μ_{LL} must increase to maintain equilibrium.

- Equation (13) also suggests that thermodynamically immersion freezing can be described as homogeneous ice nucleation occurring at an enhanced water activity. This is because it is possible to create a path including homogeneous ice nucleation with the same change in Gibbs free energy than for heterogeneous freezing, as shown in Figure 1. This fact is used to develop an expression for the work of germ formation in immersion freezing, ΔG_{het} . To this end it is useful expressing Eq. (13) in terms of the water activity. Using the equilibrium between bulk liquid and ice as the reference state, $\Delta\mu_s$, can be written in the form (Kashchiev, 2000; Barahona, 2014),

$$\Delta\mu_s = -k_B T \ln \left(\frac{a_w}{a_{w,eq}} \right), \quad (14)$$

- 20 where $a_{w,eq}$ is the equilibrium water activity between liquid and ice. Similarly, introducing the definitions,

$$\mu_w = \mu_0 + k_B T \ln(a_w), \quad (15)$$

and

$$\mu_{LL} = \mu_0 + k_B T \ln(a_{w,eff}), \quad (16)$$

Equation (13) can be written in the form,

$$25 \quad a_w = a_{w,eff} \left(\frac{a_{w,eq}}{a_{w,eff}} \right)^\zeta \exp[\Lambda_E \zeta (1 - \zeta)] \quad (17)$$



where $\Lambda_E = -\frac{2}{N} \frac{T_c}{T}$, and $a_{w, \text{eff}}$ is termed the “effective water activity” and it is the value of a_w associated with the LL regions in the vicinal water. Figure 1 shows that for a particle-droplet system in equilibrium, $a_{w, \text{eff}}$ satisfies the condition,

$$\Delta G_{\text{het}}(a_w) = \Delta G_{\text{hom}}(a_{w, \text{eff}}). \quad (18)$$

Equation (18) represents a thermodynamic relation between ΔG_{het} and ΔG_{hom} . It has the advantage that ΔG_{het} can be obtained without invoking assumptions on the mechanistic details of the interaction between the particle and the ice germ, which are parameterized by ζ . Since a_w is typically the controlled variable in ice nucleation, $a_{w, \text{eff}}$ can be readily obtained by solving Eq. (17),

$$a_{w, \text{eff}} = \left(\frac{a_w}{a_{w, \text{eq}}^\zeta} \right)^{\frac{1}{1-\zeta}} \exp(-\Lambda_E \zeta). \quad (19)$$

Although ascribing ice nucleation to the LL fraction of vicinal water agrees with the decisive role of free water in the formation of ice (Wang et al., 2016), caution must be taken in considering this to be the actual mechanism of ice nucleation, which could be quite complex. Equation (18) however establishes a thermodynamic constrain for ΔG_{het} that should be met by any ice nucleation mechanism.

2.3.2 Water activity shift

By definition the thermodynamic path shown in Fig. 1 operates between two equilibrium states. The relation between ΔG_{het} and ΔG_{hom} is therefore independent of the way the system reaches $a_{w, \text{eff}}$. One can imagine two separate experiments in which the environmental conditions are set to either a_w or $a_{w, \text{eff}}$, the former resulting in heterogeneous freezing and the latter in homogeneous ice nucleation. Equation (17) implies that in any condition when heterogeneous ice nucleation is observed at $a_{w, \text{het}} = a_w$ there is a corresponding homogeneous process that would occur at $a_{w, \text{hom}} = a_{w, \text{eff}}$. Thus we can write an equivalent expression to Eq. (17), but relating the observed homogeneous and heterogeneous ice nucleation thresholds in two separate experiments,

$$a_{w, \text{het}} = a_{w, \text{hom}} \left(\frac{a_{w, \text{eq}}}{a_{w, \text{hom}}} \right)^\zeta \exp[\Lambda_E \zeta (1 - \zeta)], \quad (20)$$

This expression is only valid at the thermodynamic limit, that is when the flux of water molecules to the nascent ice germ is very large and ice nucleation is controlled by the nucleation work. The limits of such approach are analyzed in Section 3.5.

Equation (20) is useful in deriving the so-called water activity criterion, i.e., the condition that the difference $a_{w, \text{het}} - a_{w, \text{eq}}$ must be approximately constant for a given material (Koop et al., 2000; Marcolli et al., 2007). Using the approximation $1 + \ln(a_w) \approx a_w$, Eq. (20) can be linearized in the form

$$-\zeta(a_{w, \text{hom}} - a_{w, \text{eq}}) = a_{w, \text{het}} - a_{w, \text{hom}} + \Lambda_E \zeta (1 - \zeta). \quad (21)$$



After rearranging we obtain,

$$\Delta a_{w, \text{het}} = (\Delta a_{w, \text{hom}} + \zeta \Lambda_E)(1 - \zeta), \quad (22)$$

where $\Delta a_{w, \text{hom}} = a_{w, \text{hom}} - a_{w, \text{eq}}$ and $\Delta a_{w, \text{het}} = a_{w, \text{het}} - a_{w, \text{eq}}$ are the homogeneous and heterogeneous water activity shifts, respectively. $\Delta a_{w, \text{hom}}$ has been found to be approximately constant for a wide range of solutes (Koop et al., 2000); therefore Eq. (22) suggests that $\Delta a_{w, \text{het}}$ should be approximately constant since $\zeta \Lambda_E \sim 0.01$ and only depends on T . Thus, despite its simplicity the two-state model presented in Section 2.3 implies the so-called water activity criterion (Koop et al., 2000) for heterogeneous ice nucleation, giving support to the hypothesis that increasing order near the particle surface drives ice nucleation.

2.3.3 Extension of the homogeneous model to the spinodal limit

Equation (18) indicates that calculation of ΔG_{het} requires an expression for ΔG_{hom} , for which CNT will be used. Unlike in the case of heterogeneous freezing, CNT has shown considerable success in predicting homogeneous ice nucleation rates. Recently the introduction of the nongentropic nucleation framework (NNF) (Barahona, 2014, 2015) relaxes some of the key assumptions of CNT. NNF accounts for the work of “unmixing” affecting the bulk of the liquid when the ice germ is formed (Black, 2007), and, for the finite character of the ice-liquid interface hence obviating the explicit parameterization of the ice-liquid interfacial energy. Furthermore, NNF also takes into account the fact that structural transformations are required to form ice, i.e., random clustering of water molecules is not a sufficient condition to form ice and molecular rearrangement is required (Vekilov, 2010; Barahona, 2015). At the same time, NNF is still a simple framework that can be easily implemented in large scale atmospheric models and that has been shown to reproduce homogeneous freezing temperatures down to 180 K (Barahona, 2015; O and Wood, 2016).

As $\zeta \rightarrow 1$, $a_{w, \text{eff}}$ may become very large (Eq. 19). Thus, in applying a homogeneous model to the heterogeneous problem in the form described in Section 2.3.1, caution must be taken in describing the limiting condition where the size germ becomes exceedingly small, i.e., $n_{\text{hom}}^* \rightarrow 1$, representing the vanishing of the energy barrier to ice nucleation. Since for such a limiting case thermodynamic potentials are not well defined it is necessary to evaluate whether NNF is still valid. Moreover, since it is based on CNT, NNF predicts a positive ΔG_{hom} for $n = 1$, leading to inconsistency, since the formation of a monomer-sized germ should carry no work.

At the limiting condition, $n_{\text{hom}}^* = 1$, the work of nucleation is smaller than the thermal energy of the molecules, and represents the onset of spontaneous phase separation (termed “spinodal decomposition”) during nucleation. This hypothesis has been advanced by Vekilov (2010) within the framework of the two-step nucleation theory. Here it is argued that being a far-from-equilibrium process ice nucleation always carries energy dissipation. When accounted for, the apparent inconsistency in CNT at $n_{\text{hom}}^* = 1$ vanishes, since as shown below such condition is not accessible. This approach differs from previous treatments where $n_{\text{hom}}^* = 1$ is associated with a negligible driving force for nucleation; Eq. (23) is then corrected so that $\Delta G_{\text{hom}} = 0$ when $n = 1$ (Kalikmanov and van Dongen, 1993).



To account for the finite, albeit small, amount of work dissipated from the generation of entropy during spontaneous fluctuation (Barahona, 2015), a simple approach is proposed. It involves writing the work of germ formation in the form,

$$\Delta G = -n\Delta\mu_i + n^{2/3}\Phi_s + W_d \quad (23)$$

where W_d is the work lost during germ formation, assumed independent of the germ size since it results from spontaneous fluctuations occurring within the liquid phase. $\Delta\mu_i$ is the supersaturation given by

$$\Delta\mu_i = k_B T \ln \left(\frac{a_w^2}{a_{w,eq}} \right), \quad (24)$$

and Φ_s is the energy of formation of the interface, given by,

$$\Phi_s = \Gamma_w s (\Delta h_f - \Gamma_w k_B T \ln a_w), \quad (25)$$

where the constants $\Gamma_w = 1.46$ and $s = 1.105 \text{ mol}^{2/3}$ define the coverage of the ice-water interface and the lattice geometry of the ice germ, respectively, and Δh_f is the latent heat of fusion. Other symbols are defined in Table 1. Equation (23) is the well-known CNT expression for ΔG with an additional term accounting for work dissipation. However instead of the common CNT definitions of $\Delta\mu_i$ and Φ_s (Section 2.2), the NNF approach is used (Barahona, 2014).

W_d and n_{hom}^* are obtained from the conditions,

$$\Delta G|_{n_{\text{hom}}^*=1} = 0, \quad \frac{\partial \Delta G}{\partial n_{\text{hom}}^*} = 0, \quad \frac{\partial^2 \Delta G}{\partial n^2} \Big|_{n_{\text{hom}}^*=1} = 0. \quad (26)$$

The first condition expresses the fact that the formation of monomer-sized germ carries no work. The second is the common CNT condition that a stable ice germ must be in mechanical equilibrium with its environment. Additionally, the third condition ensures that $n_{\text{hom}}^* = 1$ also corresponds to the stability limit of the system where nucleation and spontaneous separation are analogous. This is referred as the spinodal point. From Eq. (23) we obtain,

$$\frac{\partial^2 \Delta G}{\partial n^2} = -\frac{2}{9} n^{-1/3} \Phi_s = 0. \quad (27)$$

Since n only attains positive values, then only the trivial solution $\Phi_s = 0$ satisfies Eq. (27). This means that the energy barrier to the formation of the ice germ vanishes at the spinodal. Using $\Phi_s = 0$ and $\Delta G|_{n_{\text{hom}}^*=1} = 0$ Eq. (23) can be solved for W_d in the form,

$$W_d = \Delta\mu_i. \quad (28)$$



Thus the minimum amount of work dissipated during nucleation should correspond to a fluctuation relaxing $\Delta\mu_i$. Since W_d is independent of n , the critical germ size, n_{hom}^* , is simply obtained from the condition of mechanical equilibrium, in the form detailed in Barahona (2014). Using Eqs. (24) and (25), this leads to,

$$n_{\text{hom}}^* = \frac{8}{27} \left[\frac{\Gamma_w s (\Delta h_f - \Gamma_w k_B T \ln a_w)}{k_B T \ln \left(\frac{a_w^2}{a_{w,\text{eq}}} \right)} \right]^3. \quad (29)$$

5 Replacing this expression within Eq. (23), and rearranging, gives the work of germ formation by homogeneous ice nucleation,

$$\Delta G_{\text{hom}} = \frac{1}{2} \Delta\mu_i (n_{\text{hom}}^* + 2). \quad (30)$$

Equation (30) only differs from the common CNT expression (Kashchiev, 2000) on the right hand side, where it is implied that nucleation in solution requires the coordination of at least two molecules, a condition that has been observed experimentally in the crystallization of proteins (Vekilov, 2010). It also suggests that non-equilibrium effects are negligible for typical conditions

10 leading to homogeneous ice nucleation where $n_{\text{hom}}^* \sim 200$ (Barahona, 2014). Moreover, the fact that $\Delta G_{\text{hom}} > 0$ even when $n_{\text{hom}}^* \rightarrow 0$, implies that ice nucleation always requires some work. Using Eq. (18) the heterogeneous work of nucleation can be readily written as,

$$\Delta G_{\text{het}}(a_w) = \left[\frac{1}{2} \Delta\mu_i (n_{\text{hom}}^* + 2) \right]_{a_w, \text{eff}}. \quad (31)$$

The result of Eqs. (30) and (31) requires further explanation since in principle an ice germ with only two molecules does
 15 not exist. Thus Eq. (30) must be interpreted in a different way. As $\zeta \rightarrow 1$, or in deeply supercooled conditions, the fraction of ice-like regions in the vicinal water becomes large. Under such a scenario the reorientation of only two molecules may be enough to initiate ice nucleation. In other words, beyond the spinodal point ice nucleation is controlled by molecular motion within already formed ice-like regions (akin to pre-clustering). For homogeneous ice nucleation this would require extreme supercooling ($T \sim 140$ K, Fig. 2). In immersion ice nucleation it may occur at higher T since the formation of a high fraction
 20 of ice-like regions in the vicinal water is facilitated by efficient INP. This aspect of the proposed theory is further explored in Section 3.

Even with the application of NNF, CNT carries the assumption that thermodynamic potentials can be defined for the ice germ. In other words n_{hom}^* should be large enough that it represents a statistical ensemble of molecules. Of course this is not the case for $n_{\text{hom}}^* = 1$, and it may cast doubt on the application of Eq. (23) to such limits. This possibility is however
 25 mitigated in two ways. Unlike CNT implementations using the interfacial tension, the NNF framework is robust for small germs. Size effects impact ΔG mostly through Φ_s since $\Delta\mu_i$ does not change substantially with the size of the system as long as microscopic reversibility can be assumed. In NNF the product $\Gamma_w s \Delta h_f$ in Eq. (25) remains relatively constant for a given T , and Φ_s is relatively insensitive to n . This is because Δh_f decreases with n as the total cohesive energy of the germ is inversely



proportional to the number of molecules within the ice-liquid interfacial layer (Zhang et al., 1999; Johnston and Molinero, 2012). At the same time, the product Γ_{ws} , i.e., the ratio of the number of surface to interior molecules in the germ (Barahona, 2014; Spaepen, 1975) should increase for small ice germs offsetting the decrease in Δh_f . Such behavior is supported by MD simulations (Johnston and Molinero, 2012). Equation (25) thus remains valid for small germs. A second mitigating factor is discussed in Section 3.2 where it is shown that conditions leading to $n^* \approx 1$ are rare in the atmosphere, and, J_{het} is independent of n^* for very small germs.

Finally, to complete the thermodynamic description of ice nucleation near a particle-liquid interface it is necessary to specify the critical separation temperature defined in Eq. (10). The key to finding T_c , is recognizing that it corresponds to the stability limit defined by the condition $\frac{\partial^2 \Delta G}{\partial n^2} = 0$, which also defines a global minimum for ΔG_{het} . This behavior is analyzed in Fig. 2. As T decreases $\Delta \mu_i$ increases, decreasing n_{hom}^* and ΔG_{het} . However for $n_{\text{hom}}^* < 2$, the tendency is reversed and ΔG_{het} becomes proportional to $\Delta \mu_i$ and independent of n^* . For a given T there is a critical value of $\zeta = \zeta_c$ around which ΔG_{het} is minimum. This indicates that T_c should correspond to the temperature at which ΔG_{het} has a minimum for $\zeta_c = 0.5$. Figure 2 shows that this occurs around $T \sim 220$ K. In fact, combining Eqs. (19) and (31) it is possible to iteratively calculate, $T_c = 219.802$ K. Figure 2 also suggests that $\zeta = \zeta_c$ represents the transition between two thermodynamic regimes. This is analyzed in Section 3.2.

2.4 Kinetics of immersion freezing

Almost every theoretical approach to describe the effect of INP on ice formation focuses on the thermodynamics of ice nucleation. However as discussed in Section 2.1, the increased order and the no-slip condition near the surface of the particle, both of which increase the viscosity of vicinal water, imply that the immersed particle modifies the flux of water molecules to the nascent ice germ, hence the kinetics of ice germ growth. This is generally neglected in nucleation theory (e.g., Zobrist et al., 2007; Khvorostyanov and Curry, 2004b; Ickes et al., 2017). In this section a heuristic model is proposed to account for such effects.

The heterogeneous ice nucleation rate is given by the product of the equilibrium concentration of supercritical clusters and the flux of water molecules to the ice germ (Kashchiev, 2000),

$$J_{\text{het}} = C_0 Z f_{\text{het}}^* \exp\left(-\frac{\Delta G_{\text{het}}}{k_B T}\right), \quad (32)$$

where C_0 is the monomer concentration, f_{het}^* is the impingement factor for heterogeneous ice nucleation, and Z is the Zeldovich factor given by (Kashchiev, 2000),

$$Z = \left[\frac{\Delta G_{\text{het}}}{3\pi k_B T (n^*)^2} \right]^{1/2}. \quad (33)$$

where $n^* = [n_{\text{hom}}^* + 2]_{a_w, \text{eff}}$. Other symbols are defined in Table 1. In writing Eq. (32) it is assumed that interface transfer is the dominant mechanism of ice germ growth.



The impingement factor, f_{het}^* , is the frequency of attachment of water molecules to the ice germ. For homogeneous ice nucleation it is controlled by the bulk diffusion coefficient and the work dissipated during molecular transfer across the interface (Barahona, 2015), i.e.,

$$f_{\text{hom}}^* = \frac{D_{\infty} \Omega}{v_w d_0} \left[1 + \left(\frac{a_w}{a_{w,\text{eq}}} \right)^{n_t} \right]^{-1}, \quad (34)$$

- 5 where D_{∞} the bulk self-diffusion coefficient of water, Ω the surface area of the germ, v_w and d_0 the molecular volume and diameter of water, respectively, and $n_t = 16$ is the number of possible trajectories in which water molecules incorporate to the ice lattice. Equation (34) differs from common CNT expressions in that it takes into account that molecular rearrangement is required to facilitate the incorporation of water molecules to the growing ice germ, leading to energy dissipation (Barahona, 2015).
- 10 As outlined in Section 2.1 it is likely that the same mechanism that facilitates ice nucleation also controls the dynamic behavior of the environment around the particle. Thus, for heterogeneous ice nucleation f_{het}^* must be a function of ζ . This is represented by scaling in f_{hom}^* the form,

$$f_{\text{het}}^* = f_{\text{hom}}^* \Upsilon(\zeta). \quad (35)$$

- To derive an expression for $\Upsilon(\zeta)$ the relaxation theory proposed by Adam and Gibbs (1965) (hereinafter, AG65) is employed.
- 15 According to AG65, relaxation and diffusion in supercooled liquids require the formation of cooperative regions (CRs). The probability of such a rearrangement (i.e., the transition probability) is determined by the size of the smallest CR. Following a statistical mechanics treatment and assuming that each CR interacts weakly with the rest of the system, the authors derived the following expression for the average transition probability,

$$\bar{W} \propto \exp\left(-\frac{A}{TS_c}\right), \quad (36)$$

- 20 where A represents the product of the minimum size of a CR in the liquid and the energy required to displace water molecules from their equilibrium position in the bulk, and S_c is the configurational entropy. Since A is approximately constant, the mobility of water molecules is controlled by S_c . Such a behavior has been confirmed in molecular dynamics simulations and experimental studies (e.g., Scala et al., 2000; Debenedetti and Stillinger, 2001).

- Since f_{het}^* is proportional to the mobility of water molecules across the ice-liquid interface (Barahona, 2015; Kashchiev, 25 2000), hence to their transition probability, the scaling function introduced in Eq. (35) can be written in the form,

$$\Upsilon(\zeta) = \frac{\bar{W}_{\text{vc}}}{\bar{W}}, \quad (37)$$



where \bar{W}_{vc} and \bar{W} are the average transition probabilities in the vicinity of the particle and in the bulk of the liquid, respectively. Using Eq. (36), Eq. (37) can be written as,

$$\Upsilon(\zeta) = \exp\left[-\frac{A}{TS_{c,0}}\left(\frac{S_{c,0}}{S_c} - 1\right)\right], \quad (38)$$

where $S_{c,0}$ represents the value of S_c in the absence of an immersed particle (i.e., $\zeta = 0$). Equation (38) implies that the flux of molecules to the ice germ during immersion freezing is controlled by the configurational entropy of vicinal water.

The usage of Eq. (38) requires developing an expression for S_c . This is done under the assumption that the flux of water molecules to the nascent ice germ depends mostly on the fraction of LL regions in the vicinal water, that is, only molecules not participating in ice-like regions are mobile enough to diffuse to the ice germ (Stanley and Teixeira, 1980). This reduces the number of configurations available to the vicinal water, so that S_c is scaled in the form $S_c \sim S_{c,0}(1-\zeta)$. Also, to be incorporated in the ice germ water molecules should be displaced from their equilibrium position in the vicinity of the immersed particle, i.e., they should be “unmixed” from the vicinal water. Adding these contributions we obtain,

$$S_c = S_{c,0}(1-\zeta) + s_w - s_{LL} \quad (39)$$

where s_{LL} and s_w are the molar entropies of LL and water, respectively. Using Eq. (13), the last two terms of Eq. (39) can be written as,

$$s_w - s_{LL} = -\zeta \frac{\Delta\mu_s}{T} + \frac{h_w - h_{LL}}{T} - \frac{g^E}{T}. \quad (40)$$

where h_{LL} and h_w are the molar enthalpies of the bulk liquid and the LL regions, respectively. The last two terms on the right side of Eq. (40) should cancel out since in regular solutions the excess energy results mostly from enthalpy changes during mixing (Holten et al., 2013) (Section 2.3). With this, and using Eq. (14), the configurational entropy of vicinal water molecules can be approximated as,

$$S_c = S_{c,0}(1-\zeta) + \zeta k_B \ln\left(\frac{a_w}{a_{w,eq}}\right). \quad (41)$$

Introducing this expression into Eq. (38) and rearranging we obtain,

$$\Upsilon(\zeta) = \exp\left\{-\frac{A}{TS_{c,0}}\left[\frac{\zeta(1-\sigma_E)}{1-\zeta(1-\sigma_E)}\right]\right\}, \quad (42)$$

where $\sigma_E = S_{c,0}^{-1} k_B \ln\left(\frac{a_w}{a_{w,eq}}\right)$. The self-diffusivity of water is proportional to the transition probability, and can be expressed in the form $D_\infty \sim D_0 \bar{W}$ where D_0 is a constant. Thus an equivalent expression to Eq. (42) can be written in the form,

$$\Upsilon(\zeta) = \left(\frac{D_\infty}{D_0}\right)^{\frac{\zeta(1-\sigma_E)}{1-\zeta(1-\sigma_E)}}, \quad (43)$$



Equation (43) represents the effect of the immersed particle on the rate of growth of the ice germ. For $\zeta = 0$, $D = D_\infty$, i.e., the particle does not affect the flux of water molecules to the nascent ice germ. However when $\zeta \rightarrow 1$, $D \propto \exp(-1/\sigma_E)$; since $\sigma_E \sim 0.01$, interface transfer becomes severely limited.

Finally, collecting terms and replacing Eqs. (34), (35) and (43) into Eq. (32), we obtain for the heterogeneous nucleation
5 rate,

$$J_{\text{het}} = \frac{Z D_\infty \Omega}{a_0 v_w a_0} \left(\frac{D_\infty}{D_0} \right)^{\frac{\zeta(1-\sigma_E)}{1-\zeta(1-\sigma_E)}} \exp\left(-\frac{\Delta G_{\text{het}}}{k_B T}\right) = J_0 \exp\left(-\frac{\Delta G_{\text{het}}}{k_B T}\right), \quad (44)$$

where J_0 is the preexponential factor and ΔG_{het} is given by Eq. (31). In writing Eq. (44) it has been assumed that $C_0 = a_0^{-1}$ being a_0 the average cross-sectional area of a water molecule. This indicates that the particle has a well-defined surface area and that most of the molecules incorporated into the ice germ reside near the liquid-particle interface.

10 2.5 The role of active sites

In some materials ice is formed preferentially in the vicinity of surface patches that provide some advantage to ice nucleation, commonly referred as active sites. The existence of active sites have been established experimentally for deposition ice nucleation (i.e., ice nucleation directly from the vapor phase) (Kiselev et al., 2017), and there is also evidence that they may be important for immersion freezing (e.g., Murray et al., 2012). In the classical view active sites have the property of locally
15 reducing n^* and ΔG_{het} , increasing J_{het} . In the so-called singular hypothesis $J_{\text{het}} \rightarrow \infty$ at each active site. In the modern interpretation each active site has an associated characteristic temperature at which it nucleates ice with some variability due to “statistical fluctuations” in the germ size (Vali, 2014). Some approaches to describe immersion freezing account for the existence of active sites by assuming distributions of contact angles for each particle. Hence each active site is assigned a characteristic contact angle instead of a characteristic temperature (e.g., Ickes et al., 2017).

20 The view of the role of active sites as capable of locally decreasing ΔG_{het} relies heavily on an interpretation of immersion freezing that mimics ice nucleation from the vapor phase (Fig. 3a). However it may be too simple for ice formation within the liquid phase. For example, it is implicitly assumed that the active site brings molecules together, similar to an adsorption site. However a particle immersed within a liquid is already surrounded by water molecules (Fig. 3b). In fact, nascent ice structures are associated with low density regions within the liquid (Bullock and Molinero, 2013). Thus the active site should
25 be able to “pull molecules apart” instead of bringing them together. This creates a conceptual problem. To locally reduce ΔG_{het} active sites should be able to maintain water molecules in a different thermodynamic state than the rest of the liquid. In other words, they would have the unusual property of creating a thermodynamic barrier maintaining their surrounding water in a non-equilibrium state. Such situation is unlikely in immersion freezing.

The concept of local nucleation rate also presents some difficulties. In the strict sense J_{het} is the velocity with which the size
30 distribution of molecular clusters in an equilibrium population crosses the critical size (Kashchiev, 2000). The domain of such a distribution is the whole volume of the liquid. It then becomes apparent that only a single value of J_{het} can be defined for a



continuous liquid phase, independently of where the actual nucleation process is occurring, since no permanent spatial gradients of T or concentration exist within equilibrium systems. Having otherwise implies that parts of the system would need to be maintained in a non-equilibrium state, having their own cluster size distribution. This requires the presence of non-permeable barriers within the liquid, a condition not encountered in immersion freezing. Similarly, the characteristic temperature of an active site is an unmeasurable quantity since a system in equilibrium has the same temperature everywhere. Hence it would be impossible to distinguish whether the particle as a whole or only the active site must reach certain temperature before nucleation takes place.

These difficulties can be reconciled if instead of promoting nucleation through a thermodynamic mechanism, active sites provide a kinetic advantage to ice nucleation. A way in which this can be visualized is shown in Fig. 3b. The vicinal water is in equilibrium with the particle, and exhibits a larger degree of ordering near the interface. Since in immersion freezing the formation of ice in the liquid depends on molecular rearrangement rather than clustering, the active site should produce a transient structural transformation that allows the propagation of ice. These sites would be characterized by defects where templating is not efficient allowing greater molecular movement hence facilitating restructuring. Their presence is guaranteed since particles are never uniform at the molecular scale. In this view active sites create ice by promoting fluctuation instead of by locking water molecules in a strict configuration. It implies that for uniform systems (e.g., a single droplet with a single particle) ΔG_{het} depends on the equilibrium between the particle and the vicinal water and active sites enhance fluctuation around specific locations. This obviates the need for the hypothesis of a well-defined characteristic temperature for each active site. It however does not mean that active sites are transient. They are permanent features of the particle and should have a reproducible behavior, inducing ice nucleation around the same place in repeated experiments (e.g., Kiselev et al., 2017).

Within the framework presented above, there can only be one J_{het} defined in the droplet volume. The presence of active sites introduces variability in J_0 instead of ΔG_{het} . The latter is determined by the thermodynamic equilibrium between the particle and its vicinal water. Although the theory presented here does not account for internal gradients in the droplet-particle system, in practice it is likely that the that the observed J_{het} corresponds to the most active site in the particle. Variability in J_{het} would be introduced by fluctuation in the cluster size distribution in the liquid and from multiplicity of active sites in the particle. In this sense the proposed view is purely stochastic.

3 Discussion

3.1 Thermodynamic freezing temperature

To analyze the effect of the immersed particle on the thermodynamics of ice nucleation the concept of “Thermodynamic Freezing Temperature”, $T_{f,\text{eq}}$, is introduced, defined as the equilibrium temperature between the ice germ and the droplet. It differs from the experimentally measured freezing temperature, T_f , in that the latter is defined at some value of J_{het} . When $\frac{dJ_{\text{het}}}{dT}$ is large, as for example in homogeneous ice nucleation, T_f approximates $T_{f,\text{eq}}$. This concept is useful since the thermodynamics on ice nucleation can be analyzed in terms of $T_{f,\text{eq}}$, independently of any prescribed J_{het} threshold.



An example of this is the water activity criterion, Eq. (20). Since it results from an equilibrium relation, it represents a constraint between $T_{f,eq}$ (instead of T_f) and a_w . This is shown in Fig. 4. For $\zeta = 0$, $T_{f,eq}$ coincides by design with the homogeneous freezing line and it is calculated setting $\Delta a_{w,hom} = 0.304$ (Barahona, 2014). Curves for $\zeta > 0$ align with constant water activity shifts to $a_{w,eq}$, as exemplified by the two lines drawn using constant values of $\Delta a_{w,het} = 0.05$ and $\Delta a_{w,het} = 0.20$.

5 As $\zeta \rightarrow 1$, $T_{f,eq}$ lies closer to the thermodynamic equilibrium. Constant $\Delta a_{w,het}$ has been reported in several studies (e.g., Zuberi et al., 2002; Zobrist et al., 2008; Alpert et al., 2011; Knopf and Alpert, 2013). Thus the fact that such behavior can be reproduced by Eq. (20) validates the regular solution approximation of Eq. (12). It also supports the idea that the effect of the immersed particle on $T_{f,eq}$ can be explained as relative increase in the “ice-like” character of the vicinal water.

3.2 Ice nucleation regimes

10 A consequence of the linkage between the properties of vicinal water and ΔG_{het} is the existence of distinct nucleation regimes. This was mentioned in Section 2.3.3 and here it is explored in detail. Recall from Fig. 2, that ΔG_{het} passes by a minimum at ζ_c defined by the condition $\frac{\partial^2 \Delta G_{het}}{\partial n^2} = 0$. Figure 5, (right panel) shows a similar behavior but maintaining ζ constant instead of T . It shows that there is a temperature, T_s , at which ΔG_{het} is minimum. For $T > T_s$ ΔG_{het} increases with increasing T because n^* increases, as shown in Fig. 5, (left panels). This is the typical behavior predicted by CNT hence such regime will be termed

15 “germ-forming”.

On the other hand, for $T < T_s$, ΔG_{het} decreases with increasing T . In this regime n^* remains almost constant at very low values, ΔG_{het} is small and results mostly from the dissipation of work. Ice nucleation does not proceed by the formation of an ice germ but rather by the propagation of small fluctuations in the vicinity of pre-formed ice-like regions. Therefore it is controlled by diffusion of water molecules to such regions rather than by ΔG_{het} . This is akin to a spinodal decomposition

20 process (Cahn and Hilliard, 1958) and will be termed “spinodal ice nucleation”. It is however not truly spinodal decomposition since it requires a finite, albeit small, amount of work to occur.

In principle all INPs are capable of nucleating ice in both regimes. However depending on ζ , one of them may lie outside the $233 \text{ K} < T < 273 \text{ K}$ range where immersion freezing occurs. For example, for $\zeta = 0.1$, Fig. 5, right panel, suggests that the minimum in ΔG_{het} occurs at $T_s < 220 \text{ K}$. Since homogeneous ice nucleation should occur above this temperature, the

25 spinodal regime cannot be observed for an INP characterized by $\zeta = 0.1$. Thus these particles would always nucleate ice in the classical germ-forming regime ($T > T_s$). Since in this regime ΔG_{het} increases very rapidly with T (and J_0 is large, Section 3.3), the observed freezing temperature would be close to $T_{f,eq}$. The situation is however different for $\zeta = 0.9$, since $T_s \approx 270 \text{ K}$. For these INP ice formation likely occurs in the spinodal regime ($T < T_s$). In this case ΔG_{het} is very low and decreases slightly with increasing T , indicating that the thermodynamic barrier to nucleation is virtually removed. Ice formation is almost

30 entirely controlled by kinetics and it is likely that T_f differs from $T_{f,eq}$.

The existence of the spinodal nucleation regime raises a complication in the analysis of freezing experiments. That is, T_f may correspond to two very different INP. To show this the values of ΔG_{het} and n^* corresponding to $J_{het} = 10^{12} \text{ m}^{-2} \text{ s}^{-1}$ are shown in Fig. 5, black lines. Since the same ΔG_{het} may correspond to two INP with different ζ , these lines form semi-closed curves when plotted against temperature. The upper branch (with high ΔG_{het}) corresponds to the germ-forming regime and



the lower branch to the spinodal regime. This picture is further convoluted by the fact that high ζ also implies strong kinetic limitations during ice nucleation, as discussed in Section 3.4.

3.3 Preexponential Factor

Besides the effect of the particle on the thermodynamics of vicinal water, hence on ΔG_{het} , J_{het} is also strongly influenced by the modification of the flux of water molecules to the ice germ (Section 2.4). Mathematically this is expressed in terms of the preexponential factor J_0 . In general J_0 varies with T . In the absence of a immersed particle ($\zeta = 0$) the sensitivity of J_0 to T is determined by D_∞ (Barahona, 2015). Thus J_0 increases with T because water molecules increase their mobility, and because as the system moves closer to equilibrium less work is dissipated during interface transfer. Still, J_0 only increases by about two orders of magnitude between 220 K and 273 K (Fig. 6, $\zeta = 0$).

Figure 6 shows that for $\zeta < 0.5$, J_0 follows essentially the same behavior as for $\zeta = 0$, increasing slightly with T . This suggests that for $\zeta < 0.5$ the particle has a limited effect on the mobility of vicinal water and enough configurations are available to the system (i.e., S_c is large enough) so that the transition probability remains relatively constant, i.e., $\Upsilon(\zeta) \sim 1$. The dynamics of water around these particles would be reasonably well described by assuming a negligible effect of the particle on J_0 , as done in CNT.

However as ζ increases the presence of the particle tends to significantly decrease J_0 . S_c is reduced (Eq. 41) due to limitations in the number of configurations available that can form cooperative regions, hence $\Upsilon(\zeta)$ and D become small. As a result, for $\zeta > 0.5$, and particularly for $\zeta > 0.8$, J_0 decreases strongly with increasing T . For $\zeta > 0.99$ J_0 decreases by more than 30 orders of magnitude from 220 K to 273 K, i.e., molecular transport nearly stops. Ice nucleation may not be possible at such extreme, despite the fact that these particles very efficiently reduce ΔG_{het} ; water may remain in the liquid state at very low temperature. Such an effect has been experimentally observed in some biological systems (Wolfe et al., 2002).

3.4 Nucleation Rate

The discussion above indicates that J_{het} is determined by two competing effects. Particles highly efficient at decreasing ΔG_{het} also decrease the rate of interfacial diffusion to the point where they may effectively prevent ice nucleation. On the other hand, INP with low ζ do not significantly affect J_0 however they also have a limited effect on ΔG_{het} . This is confounded with the presence of two thermodynamic nucleation regimes, where ΔG_{het} may be large and increases with T (“germ-forming”), and another one where ΔG_{het} is very small and decreases as T increases (“spinodal nucleation”).

This picture can be simplified since within the range 233 K $< T < 273$ K, where immersion freezing occurs, INP with $\zeta > 0.7$ are at the same time more likely to nucleate ice in the spinodal regime and to exhibit strong kinetic limitations. Similarly for $\zeta < 0.6$ the transition to spinodal nucleation occurs below 233 K (Fig. 2). These INP tend to nucleate ice in the germ-forming regime and without significantly affecting J_0 . Thus the thermodynamic regimes introduced in Section 3.2 loosely correspond to dynamical regimes. Roughly, ice nucleation in the spinodal regime is controlled by dynamics and in the germ-forming regime it is controlled by thermodynamics. This is a useful approximation but it should be used with caution.



Even in the germ-forming regime the particle affects the dynamics of interfacial transfer to some extent. Similarly, in the spinodal regime ΔG_{het} is small, but finite.

J_{het} in the germ-forming regime resembles closely the behavior predicted by CNT since ΔG_{het} and $\frac{d\Delta G_{\text{het}}}{dT}$ are large (Fig. 5), and J_0 is relatively unaffected by the particle. Thus for $\zeta < 0.6$ it is always possible to find a contact angle (typically between 40° and 100°) that results in overlap between J_{het} and $J_{\text{het,CNT}}$ (Fig. 7). This is also true for $a_w = 0.9$ although the approximation to the equilibrium temperature signals a steeper $J_{\text{het,CNT}}$ than J_{het} , with the former peaking at higher values. Since $\frac{dJ_{\text{het}}}{dT}$ is large, J_{het} shows threshold behavior. This is characteristic of freezing mediated by some dust species like Chlorite and Montmorillonite (Murray et al., 2012; Hoose and Möhler, 2012).

The behavior of J_{het} for $\zeta > 0.7$, corresponding largely to spinodal nucleation, departs significantly from CNT. J_{het} is still comparable to $J_{\text{het,CNT}}$, but increases more slowly with decreasing T (Fig. 7). This is a result of the dynamic control of ice nucleation since ΔG_{het} is small and J_{het} mainly depends on J_0 . Since in CNT J_0 is not linked to the properties of the immersed particle, there is no value of θ that would produce overlap between J_{het} and $J_{\text{het,CNT}}$. Hence spinodal ice nucleation cannot be reproduced using CNT.

One may be tempted to assign nucleation regimes based on the values of J_{het} or T_f . This would be incorrect. Figure 7 shows that in both regimes, J_{het} may reach substantial values, hence T_f may cover the entire range $233 \text{ K} < T < 273 \text{ K}$. In fact, J_{het} curves with $\zeta > 0.7$ tend to cross those with $\zeta < 0.7$ (Fig. 7, left panels). As a consequence, two INP characterized by very different ζ can have the same freezing temperature. To discern whether T_f corresponds to an INP nucleating ice in the spinodal or the germ-forming regime it is necessary to measure $\frac{dJ_{\text{het}}}{dT}$ along with T_f .

3.5 Application to the water activity-based nucleation rate

To exemplify how each nucleation regime leads to a particular behavior of J_{het} , we will analyze the link between $\Delta a_{w,\text{het}}$ and ζ proposed in Eq. (22). $\Delta a_{w,\text{het}}$ has been determined in several studies and in principle these measurements can be used to predict J_{het} (e.g., Zobrist et al., 2008; Knopf and Alpert, 2013). Rearranging Eq. (22) we obtain,

$$\zeta^2 - \zeta \left(1 - \frac{\Delta a_{w,\text{hom}}}{\Lambda_E} \right) - \left(\frac{\Delta a_{w,\text{hom}} - \Delta a_{w,\text{het}}}{\Lambda_E} \right) = 0. \quad (45)$$

Since Λ_E and $\Delta a_{w,\text{hom}}$ are known, $\Delta a_{w,\text{het}}$ can be used to estimate ζ . Note that Λ_E is temperature dependent (Eq. 17) and using a fixed $\Delta a_{w,\text{het}}$ implies a slight dependency of ζ on T .

To test Eq. (45) the data for Leonardite (LEO) and Pawokee Peat (PP) particles (humic-like substances) obtained by Rigg et al. (2013) are used. The authors reported $\Delta a_{w,\text{het}} = 0.2703$ for LEO and $\Delta a_{w,\text{het}} = 0.2466$ for PP. These values are assumed to be independent of a_w and T with an experimental error in $\Delta a_{w,\text{het}}$ of 0.025. J_{het} for both materials is depicted in Fig. 8. Since J_{het} was obtained from two different samples and from repeated freezing and melting experiments these results represent actual nucleation rates. Application of Eq. (45) over the $T = 210 \text{ K} - 250 \text{ K}$ range results in $\zeta = 0.053 - 0.058$ for LEO and $\zeta = 0.092 - 0.101$ for PP. Within this temperature range these values correspond to the germ-forming regime. Comparison



against the experimentally determined J_{het} for three different values of a_w is shown in Fig. 8. Within the margin of error there is a reasonable agreement between the modeled and the experimental J_{het} .

Figure 8, top panels, however reveals that even if J_{het} becomes significant around the values predicted by Eq. (45), $-\frac{d \ln J_{\text{het}}}{dT}$ is overestimated, particularly for PP. This raises the possibility that these INP may nucleate ice in the spinodal regime. To test this, J_{het} was fitted to the reported measurements by varying ζ within the range where spinodal nucleation would be active. To avoid agreement by design a single ζ was used for all experiments for each species resulting in $\zeta = 0.951$ for PP and $\zeta = 0.955$ for LEO (Fig. 8, bottom panels). For PP J_{het} and $-\frac{d \ln J_{\text{het}}}{dT}$ agree better with the experimental values, whereas for LEO the agreement improves at high T but worsens at low T . For both species J_{het} seems to be slightly overestimated by the theory at the lowest a_w tested. This may be due to small uncertainties in a_w that play a large role in J_{het} (as for example the assumption of a T -independent a_w (Alpert et al., 2011)). There is the possibility that the humic acid present in PP may slightly dissolve during the experiments (D. Knopf, personal communication), which would impact not only a_w but also may modify the composition of the particles, hence ζ .

The exercise above suggests that ice nucleation in PP may follow a spinodal mechanism. Using a single value of $\Delta a_{w, \text{het}}$ to predict ζ , as expressed mathematically by Eq. (45), seems to work for LEO. Since Eq. (45) represents a thermodynamic relation between $\Delta a_{w, \text{hom}}$ and $\Delta a_{w, \text{het}}$, it is expected to work well for nucleation in the germ-forming regime (low ζ). However it fails for spinodal ice nucleation since it does not consider the effect of the particle on J_0 . Note that $\Delta a_{w, \text{het}}$ however carries important information about J_{het} (Knopf and Alpert, 2013) but for spinodal ice nucleation the relationship between $\Delta a_{w, \text{het}}$ and ζ must be more complex than predicted by Eq. (45) since kinetic limitations play a significant role. Figure 8 also shows that similar T_f can be obtained by either high or low ζ . The particular regime in which an INP nucleates ice affects mainly $-\frac{d \ln J_{\text{het}}}{dT}$, hence its sensitivity to size and cooling rate.

3.6 Limitations

It is important to analyze the effect of several assumptions introduced in Section 2 on the analysis presented here. One of the limitations of the approach used in deriving Eq. (44) is that it employs macroscale thermodynamics in the formulation of the work of nucleation. The effect of this assumption is however minimized in several ways. First, unlike frameworks based on the interfacial tension, NNF is much more robust to changes in ice germ size since the product $\Gamma_w s \Delta h_f$ remains constant (Section 2.3.1). Second, in the spinodal regime ΔG_{het} is independent of n^* and only for $T > 268$ K and in the germ-forming regime, the approach presented here may lead to uncertainty (Section 3.2). Thus Eq. (44) remains valid for most atmospheric conditions, although caution must be taken when $T_f > 268$ K. Alternatively the framework presented here could be extended to account explicitly for the effect of size on Δh_f and Γ_w (e.g., Zhang et al., 1999).

Further improvement could be achieved by implementing a more sophisticated equation of state for the vicinal water. Here a two-state assumption has been used, such that μ_{vc} is a linear combination of ice-like and liquid-like fractions. Such approximation has been used with success before (Etzler, 1983; Holten et al., 2013). However it is known that the structure of supercooled water represents an average of several distinct configurations (Stanley and Teixeira, 1980). These are in principle accounted for in the proposed approach since ζ represents a relative, not an absolute increase in the IL fraction. However there is no



guarantee that such increase can be linearly mapped in the way described in Section 2. Fortunately this would only mean in practice that the observed ζ is linked to the particular form of the equation of state used to describe the vicinal water.

Equation (44) is also blind to the surface properties of the immersed particle. The implicit assumption is that the effect of surface composition, charge, hydrophilicity and roughness on J_{het} can be parameterized as a function of ζ . The example shown in Section 3.5 suggests this is indeed the case. Making such relations explicit must however lie at the center of future development of the proposed approach. Similarly a heuristic approach was used to study the effect of irreversibility on the nucleation work. This can be improved substantially by making use of a generalized Gibbs approach (Schmelzer et al., 2006), which unfortunately may also increase the number of free parameters in the model. None of these limitations is expected to change the conclusions of this study, however they may affect the values of ζ fitted when analyzing experimental data. The approach proposed here however has the advantage of being a simple, one parameter approximation that can be easily implemented in cloud models.

4 Summary and Conclusions

Current immersion freezing theory relies on a view that mimics ice formation from the vapor, neglecting several interactions unique to the liquid. This work develops for the first time a comprehensive approach to account for such interactions. The ice nucleation activity of immersed particles is linked to their effect on the vicinal water. It is shown that the same mechanism that lowers the thermodynamic barrier for ice nucleation also tends to decrease the mobility of water molecules, hence the interfacial transfer coefficient. The role of the particle can be understood as increasing order in the adjacent water facilitating the formation of ice-like structures. Thus, instead of being purely driven by thermodynamics, heterogeneous ice nucleation in the liquid phase is a process determined by the competition between thermodynamic and kinetic constraints to the formation and propagation of ice.

To distinguish between thermodynamic and dynamic effects on ice nucleation the concept of thermodynamic freezing temperature was introduced. The properties of vicinal water were approximated assuming a regular solution between high and low density regions, with composition defined by an aerosol specific parameter, ζ , which acts as a “templating factor” for ice nucleation. This assumption leads directly to the derivation of the so-called water activity criterion for heterogeneous ice nucleation. It also results on an identity between the homogeneous and heterogeneous work of nucleation (Eq. 18) implying that by knowing an expression for ΔG_{hom} , ΔG_{het} can be readily written. This is advantageous as homogeneous ice nucleation is far better understood than immersion ice nucleation, and, because it avoids a mechanistic description of the complex interaction between the particle, the ice and the liquid. To describe ΔG_{hom} the NNF framework (Barahona, 2014) which does not use the capillarity assumption of typical CNT expressions was employed. This approach was extended to include non-equilibrium dissipation effects.

A model to describe the effect of the immersed particle on the mobility of water molecules was also developed. The model is built upon an expression for the interfacial diffusion flux that accounts for the work required for water molecules to accommodate in an ice-like manner during interface transfer. Here this expression is extended to account for the reduction in the



configurational entropy of water caused by the presence of the immersed particle, leading to increased viscosity and decreased mobility of water molecules near the particle surface. As a result, the preexponential factor tends to decrease significantly for $\zeta > 0.7$.

Accounting for the effect on the particle of the vicinal water suggests the existence of a spinodal regime in ice nucleation where a pair of molecules with orientation similar to that of bulk ice may be enough to trigger the propagation of the ice-lattice (e.g., Vekilov, 2010). However ice nucleation in this regime also tends to be strongly limited by the kinetics of interfacial transfer. Ice nucleation in the spinodal regime requires a highly efficient templating effect by the particle. Compared to the classical germ-forming regime, nucleation by an spinodal mechanism is much more limited by diffusion and exhibits a more moderate increase in J_{het} as temperature decreases. The existence of two nucleation regimes and the strong kinetic limitations occurring in efficient INP imply that the freezing temperature may be an ambiguous measure of ice nucleation activity. This is because for a given T two INP characterized by different ζ may have the same J_{het} , although with very different sensitivity to surface area and cooling rate.

The relationship between the measured shift in water activity $\Delta a_{w, \text{het}}$ and ζ was analyzed and tested using data for humic-like substances. It was found that assuming a fixed water activity shift to predict J_{het} could be appropriate for low ζ (the germ-forming regime) however may lead to overprediction of $-\frac{d \ln J_{\text{het}}}{dT}$ for high ζ . Thus the so-called water activity criterion represents an exact relation between a_w and $T_{f, \text{eq}}$, instead of T_f .

Immersion freezing research has seen a resurgence during the last decade (DeMott et al., 2011). A wealth of data is now available to test theories and new approaches to describe ice formation. To effectively doing so it is necessary to develop models that realistically capture the complexities of the liquid phase. Further development of the approach presented here will look to better describe the non-reversible aspects of nucleation as well as to establish a more complete description of the properties of the vicinal water. Application to the freezing of atmospheric aerosol requires the definition of the ice nucleation spectrum, which will be pursued in a future work. Nevertheless, the present study constitutes for first the time an approximation to the modeling of ice nucleation that links the dynamics and the kinetics of vicinal water with the ice nucleation ability of immersed particles. The approach presented here may help expanding our understanding of immersion ice nucleation and facilitate the interpretation of experimental data in situations where current models fall short. Application of these ideas in cloud models will allow elucidating under what conditions different nucleation regimes may occur in the atmosphere.

Acknowledgements. Donifan Barahona was supported by the NASA Modeling and Analysis Program, grant: 16-MAP16-0085.



References

- Adam, G. and Gibbs, J. H.: On the temperature dependence of cooperative relaxation properties in glass-forming liquids, *J. Chem. Phys.*, **43**, 139–146, 1965.
- Alpert, P., Aller, J., and Knopf, D.: Ice nucleation from aqueous NaCl droplets with and without marine diatoms, *Atm. Chem. Phys.*, **11**, 5539–5555, 2011.
- Anderson, D. M.: Ice nucleation and the substrate-ice interface, *Nature*, **216**, 563–566, <https://doi.org/10.1038/216563a0>, 1967.
- Barahona, D.: Analysis of the effect of water activity on ice formation using a new thermodynamic framework, *Atm. Chem. Phys.*, **14**, 7665–7680, <https://doi.org/10.5194/acp-14-7665-2014>, <http://www.atmos-chem-phys.net/14/7665/2014/>, 2014.
- Barahona, D.: Thermodynamic derivation of the activation energy for ice nucleation, *Atm. Chem. Phys.*, **15**, 13 819–13 831, <https://doi.org/10.5194/acp-15-13819-2015>, <http://www.atmos-chem-phys.net/15/13819/2015/>, 2015.
- Barahona, D. and Nenes, A.: Parameterization of cirrus formation in large scale models: Homogeneous nucleation, *J. Geophys. Res.*, **113**, D11 211, <https://doi.org/10.1029/2007JD009355>, 2008.
- Barahona, D. and Nenes, A.: Parameterizing the competition between homogeneous and heterogeneous freezing in cirrus cloud formation. Polydisperse ice nuclei, *Atmos. Chem. Phys.*, **9**, 5933–5948, 2009.
- Barahona, D., Molod, A., Bacmeister, J., Nenes, A., Gettelman, A., Morrison, H., Phillips, V., and Eichmann, A.: Development of two-moment cloud microphysics for liquid and ice within the NASA Goddard Earth Observing System Model (GEOS-5), *Geosc. Model Dev.*, **7**, 1733–1766, <https://doi.org/10.5194/gmd-7-1733-2014>, <http://www.geosci-model-dev.net/7/1733/2014/>, 2014.
- Barahona, D., Molod, A., and Kalesse, H.: Direct estimation of the global distribution of vertical velocity within cirrus clouds, *Scientific Reports*, **7**, 6840, <https://doi.org/10.1038/s41598-017-07038-6>, 2017.
- Bellissent-Funel, M.-C.: Water near hydrophilic surfaces, *J. Mol. Liquids*, **96**, 287–304, [https://doi.org/http://dx.doi.org/10.1016/S0167-7322\(01\)00354-3](https://doi.org/http://dx.doi.org/10.1016/S0167-7322(01)00354-3), 2002.
- Bigg, E. K.: The formation of atmospheric ice crystals by the freezing of droplets, *Q.J.R. Meteorol. Soc.*, **79**, 510–519, <https://doi.org/10.1002/qj.49707934207>, <http://dx.doi.org/10.1002/qj.49707934207>, 1953.
- Black, S.: Simulating nucleation of molecular solids, *Proc. Royal Soc. A*, **463**, 2799–2811, 2007.
- Broadley, S. L., Murray, B. J., Herbert, R. J., Atkinson, J. D., Dobbie, S., Malkin, T. L., Condliffe, E., and Neve, L.: Immersion mode heterogeneous ice nucleation by an illite rich powder representative of atmospheric mineral dust, *Atm. Chem. Phys.*, **12**, 287–307, <https://doi.org/10.5194/acp-12-287-2012>, <http://www.atmos-chem-phys.net/12/287/2012/>, 2012.
- Bullock, G. and Molinero, V.: Low-density liquid water is the mother of ice: on the relation between mesostructure, thermodynamics and ice crystallization in solutions., *Faraday Discuss.*, <https://doi.org/10.1039/C3FD00085K>, 2013.
- Cahn, J. W.: Surface stress and the chemical equilibrium of small crystals—I. The case of the isotropic surface, *Acta Metallurgica*, **28**, 1333–1338, 1980.
- Cahn, J. W. and Hilliard, J. E.: Free energy of a nonuniform system. I. Interfacial free energy, *J. Chem. Phys.*, **28**, 258–267, 1958.
- Cooke, R. and Kuntz, I.: The properties of water in biological systems, *Ann. Review Biophys. Bioeng.*, **3**, 95–126, 1974.
- Cox, S. J., Kathmann, S. M., Slater, B., and Michaelides, A.: Molecular simulations of heterogeneous ice nucleation. I. Controlling ice nucleation through surface hydrophilicity, *J. Chem. Phys.*, **142**, 184704, <https://doi.org/http://dx.doi.org/10.1063/1.4919714>, <http://scitation.aip.org/content/aip/journal/jcp/142/18/10.1063/1.4919714>, 2015.



- Cziczo, D. J., Froyd, K. D., Hoose, C., Jensen, E. J., Diao, M., Zondlo, M. A., Smith, J. B., Twohy, C. H., and Murphy, D. M.: Clarifying the Dominant Sources and Mechanisms of Cirrus Cloud Formation, *Science*, 340, 1320–1324, 2013.
- De Gennes, P.-G.: Wetting: statics and dynamics, *Rev. Modern Phys.*, 57, 827, 1985.
- Debenedetti, P. G. and Stillinger, F. H.: Supercooled liquids and the glass transition, *Nature*, 410, 259–267, 2001.
- 5 DeMott, P., Cziczo, D., Prenni, A., Murphy, D., Kreidenweis, S., Thompson, D., Borys, R., and Rogers, D.: Measurements of the concentration and composition of nuclei for cirrus formation, *Proc. Natl. Acad. Sci. USA*, 100, 14 655–14 660, 2003.
- DeMott, P. J., Prenni, A. J., Liu, X., Kreidenweis, S. M., Petters, M. D., Twohy, C. H., Richardson, M. S., Eidhammer, T., and Rogers, D. C.: Predicting global atmospheric ice nuclei distributions and their impacts on climate, *PNAS*, 107, 11 217–11 222, <https://doi.org/10.1073/pnas.0910818107>, 2010.
- 10 DeMott, P. J., Möhler, O., Stetzer, O., Vali, G., Levin, Z., Petters, M. D., Murakami, M., Leisner, T., Bundke, U., Klein, H., et al.: Resurgence in ice nuclei measurement research, *BAMS*, 92, 1623–1635, 2011.
- Diehl, K. and Wurzler, S.: Heterogeneous drop freezing in the immersion mode: model calculations considering soluble and insoluble particles in the drops, *J. Atmos. Sci.*, 61, 2063–2072, 2004.
- Drost-Hansen, W.: Structure of water near solid interfaces, *Ind. & Eng. Chem.*, 61, 10–47, 1969.
- 15 Espinosa, J., Sanz, E., Valeriani, C., and Vega, C.: Homogeneous ice nucleation evaluated for several water models, *J. Chem. Phys.*, 141, 18C529, 2014.
- Etzler, F. M.: A statistical thermodynamic model for water near solid interfaces, *J. Coll. Interf. Sci.*, 92, 43–56, 1983.
- Feibelman, P. J.: The first wetting layer on a solid, *Physics today*, 63, 34, 2010.
- Fitzner, M., Sosso, G. C., Cox, S. J., and Michaelides, A.: The Many Faces of Heterogeneous Ice Nucleation: Interplay Between Surface Morphology and Hydrophobicity, *J. Am. Chem. Soc.*, 137, 13 658–13 669, <https://doi.org/10.1021/jacs.5b08748>, 2015.
- 20 Fletcher, H.: On ice-crystal production by aerosol particles, *J. Atmos. Sci.*, 16, 173–180, 1959.
- Gettelman, A., Liu, X., Barahona, D., Lohmann, U., and Chen, C.: Climate impacts of ice nucleation, *J. Geophys. Res.*, 117, <https://doi.org/10.1029/2012JD017950>, 2012.
- Hiranuma, N., Augustin-Bauditz, S., Bingemer, H., Budke, C., Curtius, J., Danielczok, A., Diehl, K., Dreischmeier, K., Ebert, M., Frank, F., Hoffmann, N., Kandler, K., Kiselev, A., Koop, T., Leisner, T., Möhler, O., Nillius, B., Peckhaus, A., Rose, D., Weinbruch, S., Wex, H., Boose, Y., DeMott, P. J., Hader, J. D., Hill, T. C. J., Kanji, Z. A., Kulkarni, G., Levin, E. J. T., McCluskey, C. S., Murakami, M., Murray, B. J., Niedermeier, D., Petters, M. D., O’Sullivan, D., Saito, A., Schill, G. P., Tajiri, T., Tolbert, M. A., Welti, A., Whale, T. F., Wright, T. P., and Yamashita, K.: A comprehensive laboratory study on the immersion freezing behavior of illite NX particles: a comparison of 17 ice nucleation measurement techniques, *Atm. Chem. Phys.*, 15, 2489–2518, <https://doi.org/10.5194/acp-15-2489-2015>, <http://www.atmos-chem-phys.net/15/2489/2015/>, 2015.
- 30 Holten, V., Limmer, D. T., Molinero, V., and Anisimov, M. A.: Nature of the anomalies in the supercooled liquid state of the mW model of water, *J. Chem. Phys.*, 138, 174 501, 2013.
- Hoose, C. and Möhler, O.: Heterogeneous ice nucleation on atmospheric aerosols: a review of results from laboratory experiments, *Atm. Chem. Phys.*, 12, 9817–9854, <https://doi.org/10.5194/acp-12-9817-2012>, <http://www.atmos-chem-phys.net/12/9817/2012/>, 2012.
- 35 Hoose, C., Kristjansson, J., Chen, J.-C., and Hazra, A.: A classical-theory-based parameterization of heterogeneous ice nucleation by mineral dust, soot, and biological particles in a global climate model, *J. Atmos. Sci.*, 67, 2483–2503, <https://doi.org/10.1175/2010JAS3425.1>, 2010.
- Ickes, L., Welti, A., Hoose, C., and Lohmann, U.: Classical nucleation theory of homogeneous freezing of water: thermodynamic and kinetic parameters, *Phys. Chem. Chem. Phys.*, 17, 5514–5537, <https://doi.org/10.1039/C4CP04184D>, 2015.



- Ickes, L., Welti, A., and Lohmann, U.: Classical nucleation theory of immersion freezing: sensitivity of contact angle schemes to thermodynamic and kinetic parameters, *Atm. Chem. Phys.*, 17, 1713–1739, <https://doi.org/10.5194/acp-17-1713-2017>, <https://www.atmos-chem-phys.net/17/1713/2017/>, 2017.
- Johari, G., Fleissner, G., Hallbrucker, A., and Mayer, E.: Thermodynamic continuity between glassy and normal water, *J. Phys. Chem.*, 98, 4719–4725, 1994.
- Johnston, J. C. and Molinero, V.: Crystallization, melting, and structure of water nanoparticles at atmospherically relevant temperatures, *JACS*, 134, 6650–6659, <https://doi.org/10.1021/ja210878c>, 2012.
- Kalikmanov, V. I. and van Dongen, M. E. H.: Self-consistent cluster approach to the homogeneous kinetic nucleation theory, *Phys. Rev. E*, 47, 3532–3539, <https://doi.org/10.1103/PhysRevE.47.3532>, 1993.
- Kashchiev, D.: Nucleation: basic theory with applications, Butterworth Heinemann, 2000.
- Khvorostyanov, V. and Curry, J.: The theory of ice nucleation by heterogeneous freezing of deliquescent mixed CCN. Part I: critical radius, energy and nucleation rate, *J. Atmos. Sci.*, 61, 2676–2691, 2004a.
- Khvorostyanov, V. I. and Curry, J. A.: Thermodynamic theory of freezing and melting of water and aqueous solutions, *J. Phys. Chem. A*, 108, 11 073–11 085, 2004b.
- Kiselev, A., Bachmann, F., Pedevilla, P., Cox, S. J., Michaelides, A., Gerthsen, D., and Leisner, T.: Active sites in heterogeneous ice nucleation—the example of K-rich feldspars, *Science*, 355, 367–371, <https://doi.org/10.1126/science.aai8034>, 2017.
- Knopf, D. A. and Alpert, P. A.: A water activity based model of heterogeneous ice nucleation kinetics for freezing of water and aqueous solution droplets, *Faraday disc.*, 165, 513–534, 2013.
- Koop, T. and Zobrist, B.: Parameterizations for ice nucleation in biological and atmospheric systems, *Phys. Chem. Chem. Phys.*, 11, 10 839–10 850, 2009.
- Koop, T., Luo, B., Tslas, A., and Peter, T.: Water activity as the determinant for homogeneous ice nucleation in aqueous solutions, *Nature*, 406, 611–614, 2000.
- Lance, S., Shupe, M. D., Feingold, G., Brock, C. A., Cozic, J., Holloway, J. S., Moore, R. H., Nenes, A., Schwarz, J. P., Spackman, J. R., Froyd, K. D., Murphy, D. M., Brioude, J., Cooper, O. R., Stohl, A., and Burkhardt, J. F.: Cloud condensation nuclei as a modulator of ice processes in Arctic mixed-phase clouds, *Atm. Chem. Phys.*, 11, 8003–8015, <https://doi.org/10.5194/acp-11-8003-2011>, <http://www.atmos-chem-phys.net/11/8003/2011/>, 2011.
- Li, K., Xu, S., Chen, J., Zhang, Q., Zhang, Y., Cui, D., Zhou, X., Wang, J., and Song, Y.: Viscosity of interfacial water regulates ice nucleation, *App. Phys. Lett.*, 104, 101 605, <https://doi.org/http://dx.doi.org/10.1063/1.4868255>, 2014.
- Lohmann, U. and Feichter, J.: Global indirect aerosol effects: a review, *Atmos. Chem. Phys.*, 5, 715–737, 2005.
- Lupi, L., Hudait, A., and Molinero, V.: Heterogeneous Nucleation of Ice on Carbon Surfaces, *J. Am. Chem. Soc.*, 136, 3156–3164, 2014.
- Marcollì, C., Gedamke, S., Peter, T., and Zobrist, B.: Efficiency of immersion mode ice nucleation on surrogates of mineral dust, *Atmos. Chem. Phys.*, 7, 5081–5091, 2007.
- Matsumoto, M., Saito, S., and Ohmine, I.: Molecular dynamics simulation of the ice nucleation and growth process leading to water freezing, *Nature*, 416, 409–413, 2002.
- Meyers, M., DeMott, P., and Cotton, R.: New primary ice-nucleation parameterization in an explicit cloud model, *J. Appl. Meteorol.*, 31, 708–721, 1992.
- Michaelides, A. and Morgenstern, K.: Ice nanoclusters at hydrophobic metal surfaces, *Nature materials*, 6, 597–601, <https://doi.org/doi:10.1038/nmat1940>, 2007.



- Michot, L. J., Villiéras, F., François, M., Bihannic, I., Pelletier, M., and Cases, J.-M.: Water organisation at the solid–aqueous solution interface, *Comptes Rendus Geoscience*, 334, 611–631, 2002.
- Murphy, D. and Koop, T.: Review of the vapour pressures of ice and supercooled water for atmospheric applications, *Q. J. R. Meteorol. Soc.*, 131, 1539–1565, 2005.
- 5 Murray, B., O’Sullivan, D., Atkinson, J., and Webb, M.: Ice nucleation by particles immersed in supercooled cloud droplets, PCCP, p. Submitted, 2012.
- Myhre, G., Shindell, D., Breon, F.-M., Collins, W., Fuglestedt, J., Huang, J., Koch, D., Lamarque, J.-F., Lee, D., Mendoza, B., Nakajima, T., Robock, A., Stephens, G., Takemura, T., and Zhang, H.: Anthropogenic and Natural Radiative Forcing. *Climate Change 2013: The Physical Science Basis. Contribution of Working Group I to the Fifth Assessment Report of the Intergovernmental Panel on Climate Change*, book section 8, p. 659–740, Cambridge University Press, Cambridge, United Kingdom and New York, NY, USA, <https://doi.org/10.1017/CBO9781107415324.018>, www.climatechange2013.org, 2013.
- 10 Niemand, M., Möhler, O., Vogel, B., Vogel, H., Hoose, C., Connolly, P., Klein, H., Bingemer, H., DeMott, P., Skrotzki, J., and Leisner, T.: A particle-surface-area-based parameterization of immersion freezing on desert dust particles, *J. Atmos. Sci.*, 69, 3077–3092, <https://doi.org/10.1175/JAS-D-11-0249.1>, 2012.
- 15 O, K.-T. and Wood, R.: Exploring an approximation for the homogeneous freezing temperature of water droplets, *Atm. Chem. Phys.*, 16, 7239–7249, <https://doi.org/10.5194/acp-16-7239-2016>, <http://www.atmos-chem-phys.net/16/7239/2016/>, 2016.
- Phillips, V. T., Demott, P. J., Andronache, C., Pratt, K. A., Prather, K. A., Subramanian, R., and Twohy, C.: Improvements to an Empirical Parameterization of Heterogeneous Ice Nucleation and its Comparison with Observations, *J. Atmos. Sci.*, 70, 378–409, <https://doi.org/10.1175/JAS-D-12-080.1>, 2013.
- 20 Pruppacher, H. and Klett, J.: *Microphysics of clouds and precipitation*, Kluwer Academic Publishers, Boston, MA, 2nd edn., 1997.
- Reinhardt, A., Doye, J. P., Noya, E. G., and Vega, C.: Local order parameters for use in driving homogeneous ice nucleation with all-atom models of water, *J. Chem. Phys.*, 137, 194504, 2012.
- Rigg, Y. J., Alpert, P. A., and Knopf, D. A.: Immersion freezing of water and aqueous ammonium sulfate droplets initiated by humic-like substances as a function of water activity, *Atm. Chem. Phys.*, 13, 6603–6622, <https://doi.org/10.5194/acp-13-6603-2013>, <http://www.atmos-chem-phys.net/13/6603/2013/>, 2013.
- 25 Rinnert, E., Carteret, C., Humbert, B., Fragneto-Cusani, G., Ramsay, J. D., Delville, A., Robert, J.-L., Bihannic, I., Pelletier, M., and Michot, L. J.: Hydration of a synthetic clay with tetrahedral charges: a multidisciplinary experimental and numerical study, *J. Phys. Chem. B*, 109, 23745–23759, 2005.
- Rusanov, A. I.: Surface thermodynamics revisited, *Surf. Sc. Reports*, 58, 111–239, 2005.
- 30 Scala, A., Starr, F. W., La Nave, E., Sciortino, F., and Stanley, H. E.: Configurational entropy and diffusivity of supercooled water, *Nature*, 406, 166–169, 2000.
- Schmelzer, J. W., Boltachev, G. S., and Baidakov, V. G.: Classical and generalized Gibbs’ approaches and the work of critical cluster formation in nucleation theory, *The Journal of chemical physics*, 124, 194503, 2006.
- Smith, R. S. and Kay, B. D.: The existence of supercooled liquid water at 150 K, *Nature*, 398, 788–791, 1999.
- 35 Snyder, P. W., Lockett, M. R., Moustakas, D. T., and Whitesides, G. M.: Is it the shape of the cavity, or the shape of the water in the cavity?, *The European Physical Journal Special Topics*, 223, 853–891, <https://doi.org/10.1140/epjst/e2013-01818-y>, 2014.
- Spaepen, F.: A structural model for the solid-liquid interface in monatomic systems, *Acta Metallurgica*, 23, 729–743, 1975.



- Stanley, H. E. and Teixeira, J.: Interpretation of the unusual behavior of H₂O and D₂O at low temperatures: tests of a percolation model, *J. Chem. Phys.*, 73, 3404–3422, 1980.
- Tan, I., Storelvmo, T., and Zelinka, M. D.: Observational constraints on mixed-phase clouds imply higher climate sensitivity, *Science*, 352, 224–227, <https://doi.org/10.1126/science.aad5300>, 2016.
- 5 Taylor, J. H. and Hale, B. N.: Monte Carlo simulations of water-ice layers on a model silver iodide substrate: A comparison with bulk ice systems, *Physical Rev. B*, 47, 9732, 1993.
- Tester, J. W., Modell, M., et al.: *Thermodynamics and its Applications*, Prentice Hall PTR, 1997.
- Turnbull, D. and Fisher, J. C.: Rate of nucleation in condensed systems, *J. Chem. Phys.*, 17, 71–73, 1949.
- Vali, G.: Interpretation of freezing nucleation experiments: singular and stochastic; sites and surfaces, *Atm. Chem. and Phys.*, 14, 5271–5294, <https://doi.org/10.5194/acp-14-5271-2014>, <https://www.atmos-chem-phys.net/14/5271/2014/>, 2014.
- 10 Vekilov, P. G.: The two-step mechanism of nucleation of crystals in solution, *Nanoscale*, 2, 2346–2357, <https://doi.org/10.1039/C0NR00628A>, 2010.
- Wang, J., Kalinichev, A. G., and Kirkpatrick, R. J.: Effects of substrate structure and composition on the structure, dynamics, and energetics of water at mineral surfaces: A molecular dynamics modeling study, *Geochimica et cosmochimica acta*, 70, 562–582, <https://doi.org/10.1016/j.gca.2005.10.006>, 2006.
- 15 Wang, Q., Zhao, L., Li, C., and Cao, Z.: The decisive role of free water in determining homogenous ice nucleation behavior of aqueous solutions, *Scientific reports*, 6, 26 831, 2016.
- Warne, M., Allan, N., and Cosgrove, T.: Computer simulation of water molecules at kaolinite and silica surfaces, *Phys. Chem. Chem. Phys.*, 2, 3663–3668, 2000.
- 20 Wiacek, A., Peter, T., and Lohmann, U.: The potential influence of Asian and African mineral dust on ice, mixed-phase and liquid water clouds, *Atmospheric Chemistry and Physics*, 10, 8649–8667, <https://doi.org/10.5194/acp-10-8649-2010>, <http://www.atmos-chem-phys.net/10/8649/2010/>, 2010.
- Wolfe, J., Bryant, G., and Koster, K. L.: What is 'unfreezable water', how unfreezable is it and how much is there?, *CryoLetters*, 23, 157–166, 2002.
- 25 Yu, C.-J., Evmenenko, G., Richter, A., Datta, A., Kmetko, J., and Dutta, P.: Order in molecular liquids near solid–liquid interfaces, *App. Surface Sci.*, 182, 231–235, [https://doi.org/10.1016/S0169-4332\(01\)00410-X](https://doi.org/10.1016/S0169-4332(01)00410-X), 2001.
- Zhang, Z., Lü, X., and Jiang, Q.: Finite size effect on melting enthalpy and melting entropy of nanocrystals, *Physica B: Condensed Matter*, 270, 249–254, [https://doi.org/10.1016/S0921-4526\(99\)00199-4](https://doi.org/10.1016/S0921-4526(99)00199-4), 1999.
- Zheng, J.-m., Chin, W.-C., Khijniak, E., Khijniak Jr, E., and Pollack, G. H.: Surfaces and interfacial water: evidence that hydrophilic surfaces have long-range impact, *Adv. Colloid Interface Sc.*, 127, 19–27, <https://doi.org/doi.org/10.1016/j.cis.2006.07.002>, 2006.
- 30 Zobrist, B., Koop, T., Luo, B., Marcolli, C., and Peter, T.: Heterogeneous ice nucleation rate coefficient of water droplets coated by a nonadecanol monolayer, *J. Phys. Chem. C*, 111, 2149–2155, 2007.
- Zobrist, B., Marcolli, C., Peter, T., and Koop, T.: Heterogeneous ice nucleation in aqueous solutions: the role of water activity, *J. Phys. Chem. A*, 112, 3965–3975, 2008.
- 35 Zuberi, B., Bertram, A., Cassa, C., Molina, L., and Molina, M.: Heterogeneous nucleation of ice in (NH₄)₂SO₄-H₂O particles with mineral dust immersions, *Geophys. Res. Lett.*, 29, 1504, doi:10.1029/2001GL014 289, 2002.

**Table 1.** List of symbols.

a_0	Cross-sectional area of a water molecule, m^2
A_w	Phenomenological interaction parameter
a_w	Activity of water
$a_{w, \text{eff}}$	Effective water activity
$a_{w, \text{eq}}$	Equilibrium a_w between bulk liquid and ice (Koop and Zobrist, 2009)
$a_{w, v}$	Activity of water near the immersed particle
$a_{w, \text{het}}$	Thermodynamic freezing threshold for heterogeneous ice nucleation
$a_{w, \text{hom}}$	Thermodynamic freezing threshold for homogeneous ice nucleation
C_0	Monomer concentration, m^{-2}
E, T_0	Parameters of the VFT equation, 892 and 118 K, respectively (Smith and Kay, 1999)
D	Diffusion coefficient for interface transfer, $\text{m}^2 \text{s}^{-1}$
D_∞	Self-diffusion coefficient of bulk water (Smith and Kay, 1999), $\text{m}^2 \text{s}^{-1}$
D_0	Fitting parameter, $3.06 \times 10^{-9} \text{m}^2 \text{s}^{-1}$ (Smith and Kay, 1999)
d_0	Molecular diameter of water, m
f_f	Freezing fraction
f_{het}^*	Impingement factor for heterogeneous ice nucleation, s^{-1}
f_{hom}^*	Impingement factor for homogeneous ice nucleation, s^{-1}
g^E	Excess Gibbs free energy, J
G	Gibbs free energy, J
$G_{\text{liq}}, G_{\text{ice}}$	Gibbs free energy of liquid and ice, respectively, J
h_{vc}	Enthalpy of vicinal water, J
h	Planck's constant, Js
J_0	Preexponential factor $\text{m}^{-2} \text{s}^{-1}$
J_{het}	Heterogeneous nucleation rate, $\text{m}^{-2} \text{s}^{-1}$
$J_{\text{het, CNT}}$	Heterogeneous nucleation rate from CNT, $\text{m}^{-2} \text{s}^{-1}$
k_B	Boltzmann constant, J K^{-1}
N	Number of molecules in a cluster involving ice-liquid bonds, 6
N_c	Number of atoms in contact with the ice germ, $5.85 \times 10^{18} \text{m}^{-2}$ (Pruppacher and Klett, 1997)
n	Number of molecules in a cluster
n^*	Critical germ size
n_{hom}^*	Critical germ size for homogeneous ice nucleation
n_t	Number of formation paths of the transient state, 16 (Barahona, 2015)
$p_{s, w}, p_{s, i}$	Liquid water and ice saturation vapor pressure, respectively, Pa (Murphy and Koop, 2005)



Table 1. Continued.

s	Geometric constant of the ice lattice, $1.105 \text{ mol}^{2/3}$ (Barahona et al., 2014)
S_i	Saturation ratio with respect to ice
$S_{c,0}$	Configuration entropy of water*
S_c	Configuration entropy of vicinal water
T	Temperature, K
T_c	Critical separation temperature, 219.802 K
v_w	Molecular volume of water in ice (Zobrist et al., 2007), m^{-3}
$v_{w,0}$	Molecular volume of water at 273.15 K
\bar{W}, \bar{W}_{vc}	Transition probability in the bulk liquid and in the vicinal water, respectively
W_d	Work dissipated during cluster formation, J
Z	Zeldovich factor
$\Delta a_{w, \text{het}}$	$a_{w, \text{het}} - a_{w, \text{eq}}$
$\Delta a_{w, \text{hom}}$	$a_{w, \text{hom}} - a_{w, \text{eq}}, 0.304$
ΔG	Work of cluster formation, J
ΔG_{act}	Activation energy for ice nucleation, J
ΔG_{hom}	Nucleation work for homogeneous ice nucleation, J
ΔG_{het}	Nucleation work for heterogeneous ice nucleation, J
ΔG_{CNT}	Nucleation work from CNT, J
Δh_f	Heat of solidification of water, J mol^{-1} (Barahona et al., 2014; Johari et al., 1994)
$\Delta \mu_f$	Excess free energy of solidification of water, J
$\Delta \mu_i$	Supersaturation, J
Λ_E	Dimensionless interaction parameter, $-\frac{2}{N} \frac{T_c}{T}$
Φ	Energy of formation of the ice-liquid interface
Γ_w	Molecular surface excess of at the interface, 1.46 (Barahona et al., 2014; Spaepen, 1975)
γ_c	Cooling rate, $-\frac{dT}{dt}$
μ_w, μ_s, μ_{vc}	Chemical potential of water, ice and vicinal water, respectively J
ρ_w, ρ_i	Bulk density of liquid water and ice, respectively, Kg m^{-3} (Pruppacher and Klett, 1997)
σ_E	Dimensionless residual entropy
σ_{iw}	Ice-liquid interfacial energy J m^{-2} (Barahona et al., 2014)
θ	Contact angle
ζ	Templating factor
Ω_g	Ice germ surface area, m^{-2}

* From the data of Scala et al. (2000) the following fit was obtained:

$$S_{c,0} = k_B v_w / v_{w,0} (-7.7481 \times 10^{-5} T^2 + 5.5160 \times 10^{-2} T - 6.6716) \text{ (J K}^{-1}\text{) for } T \text{ between 180 K and 273 K.}$$

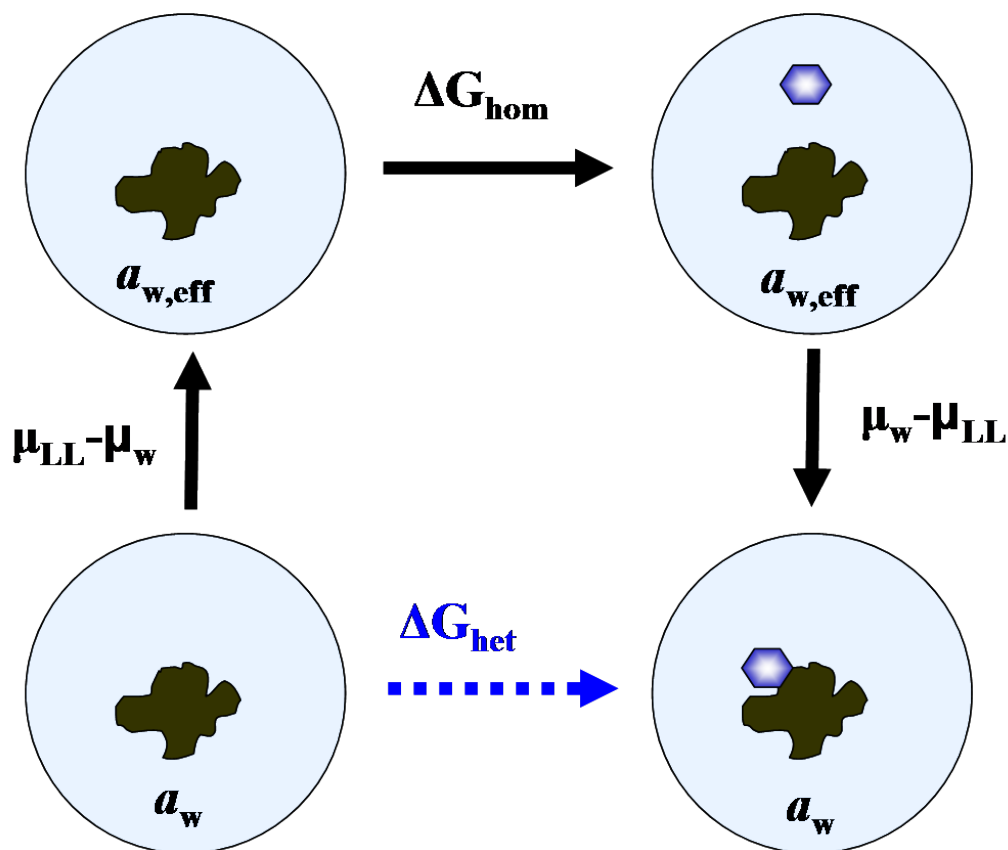


Figure 1. Diagram representing a thermodynamic path including homogeneous ice nucleation with the same work as heterogeneous freezing.

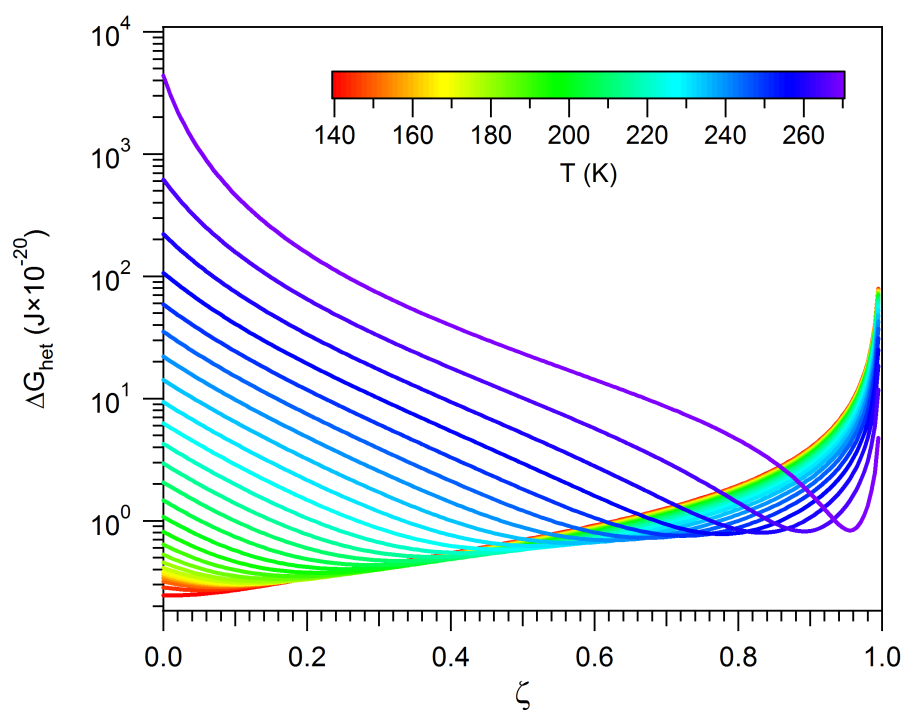


Figure 2. Work of heterogeneous ice nucleation. Color indicates different temperatures.

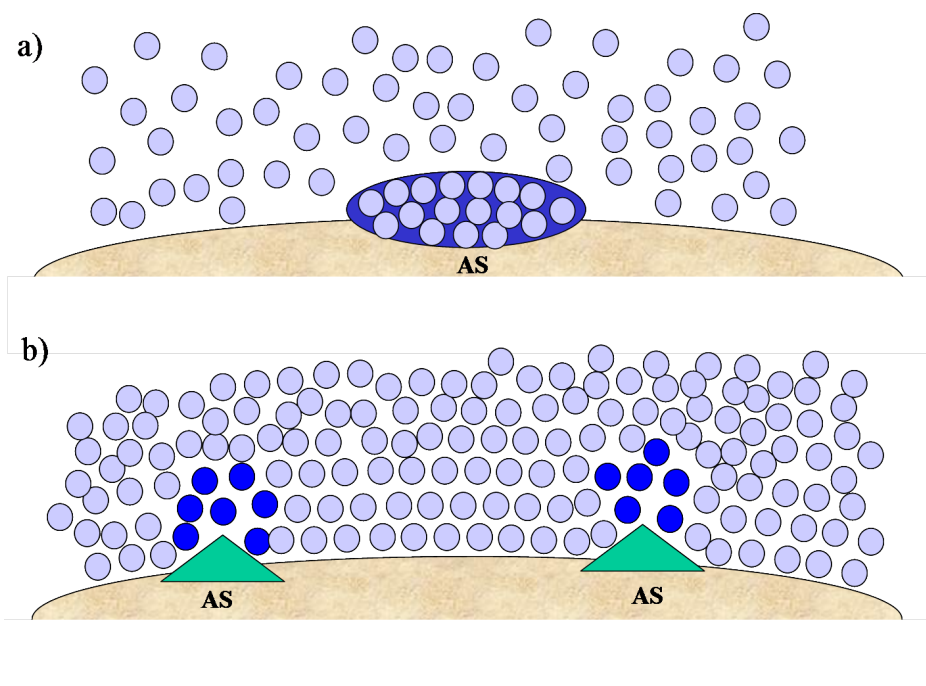


Figure 3. Different representations of immersion freezing. (a) An ice germ (dark blue) forming on an active site (AS) by random collision of water molecules (light blue). (b) Low density regions (dark blue) forming in the vicinity of active sites within a dense liquid phase (light blue).

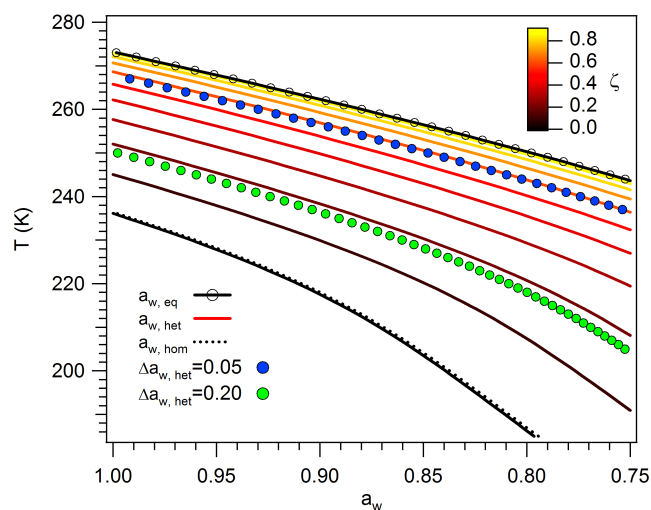


Figure 4. Thermodynamic freezing temperature as a function of water activity. Color lines correspond to $a_{w, het}$ (Eq. 22) for different values of ζ . Also shown are a_w at equilibrium and at the homogeneous freezing threshold, $a_{w, eq}$ and $a_{w, hom}$, respectively, and lines drawn applying constant water activity shifts, $\Delta a_{w, het}$, of 0.05 and 0.20.

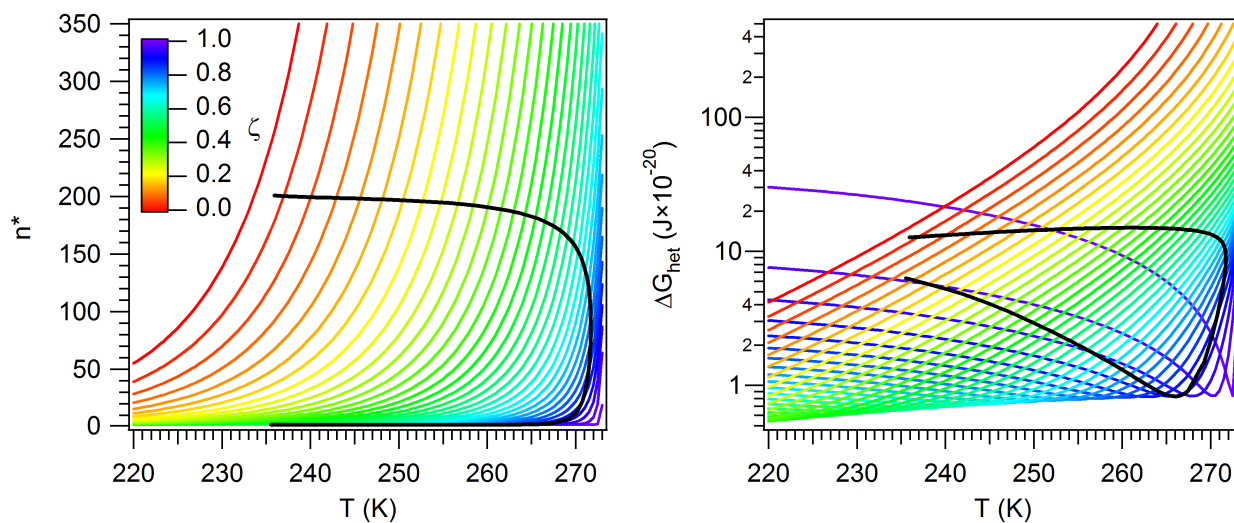


Figure 5. Critical germ size (left panel) and work of heterogeneous ice nucleation (right panels) for different values of ζ (color). Black lines correspond to constant $J_{\text{het}} = 10^{12} \text{ m}^{-2} \text{ s}^{-1}$.

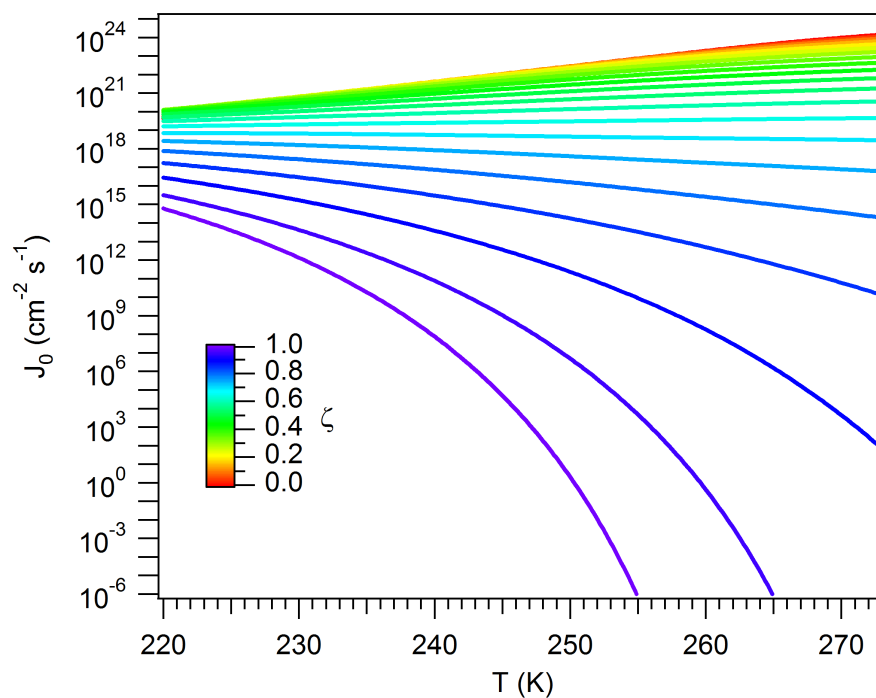


Figure 6. Preexponential factor. Color indicates different values of ζ .

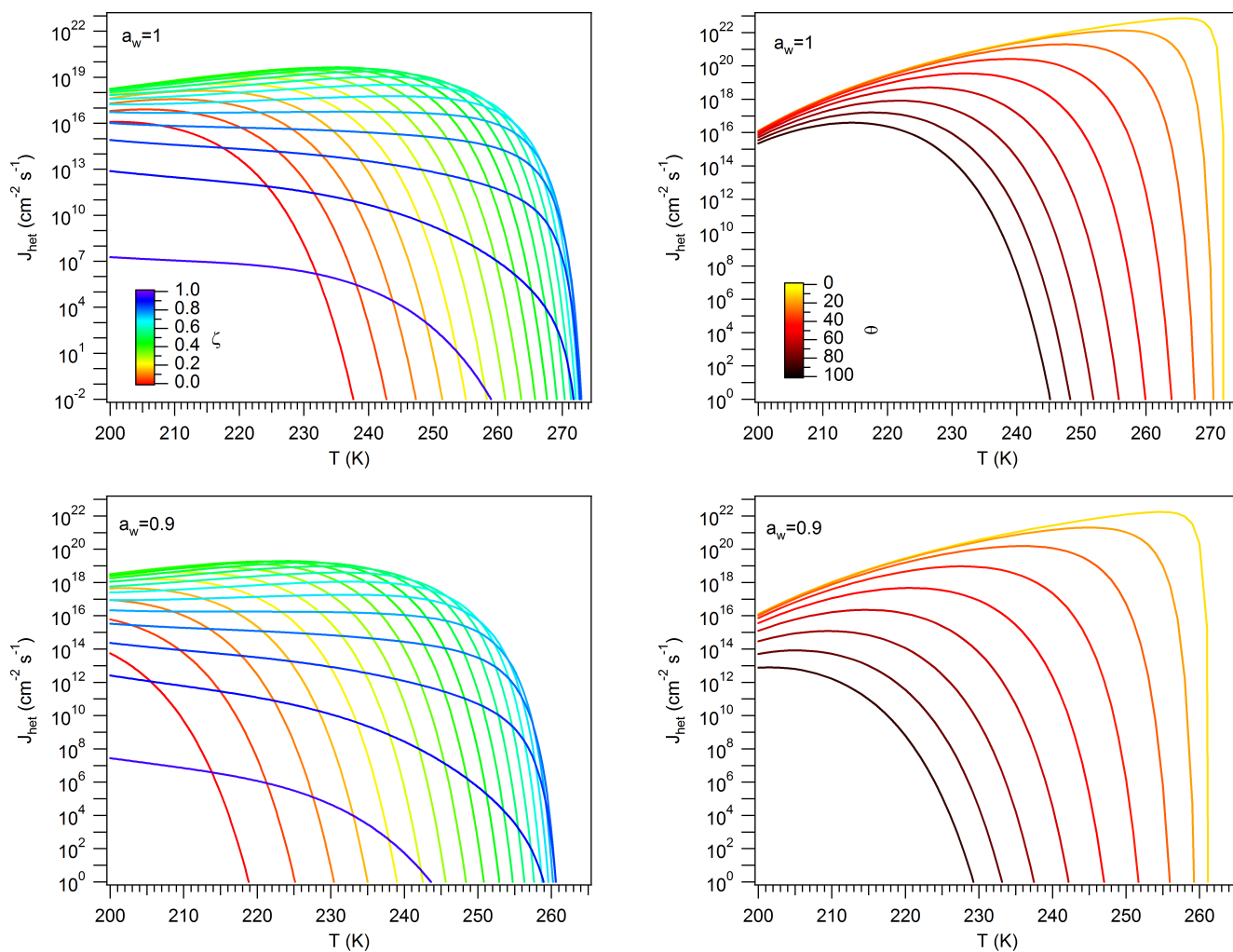


Figure 7. Ice nucleation rate calculated using Eq. (44) (left panels) and Eq. (1) (right panels) for two different values of water activity. Color corresponds to either ζ (left panels) or the contact angle (right panels).

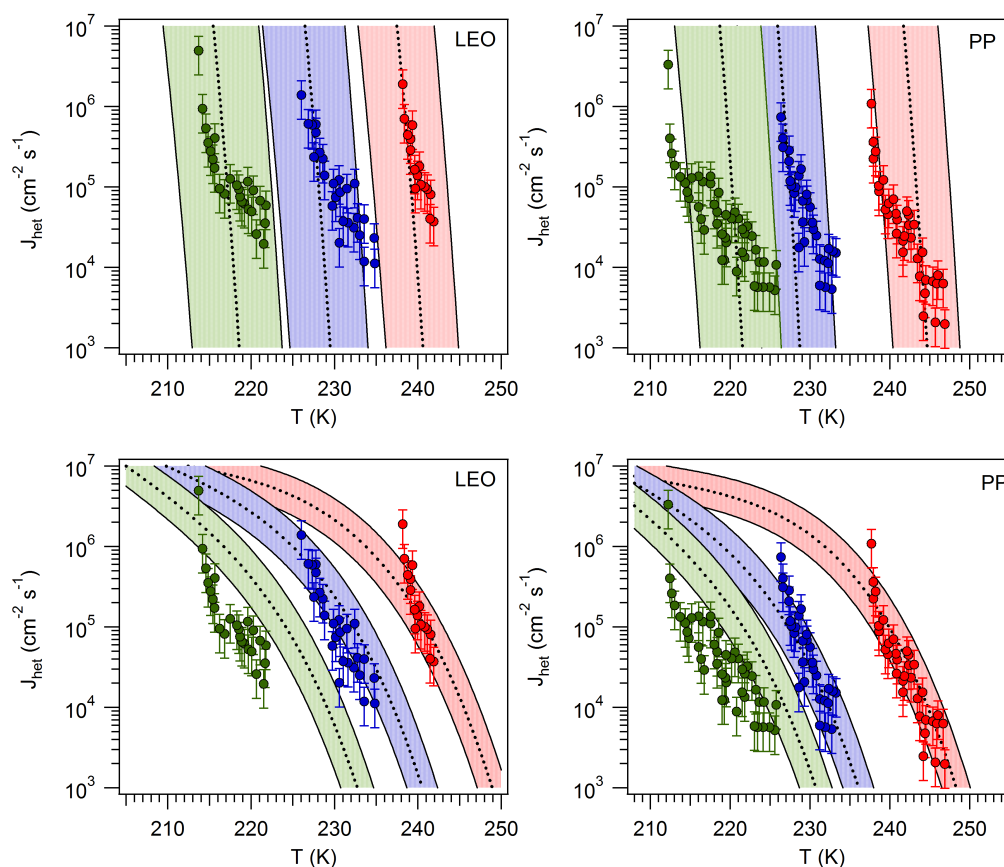


Figure 8. Top panels: Heterogeneous ice nucleation rate calculated using a constant shift in a_w (black, dotted, lines) for Leonardite (LEO $\Delta a_{w, \text{het}} = 0.2703$) and Pawokee Peat (PP, $\Delta a_{w, \text{het}} = 0.2466$) (top panels). Red, blue and green colors correspond to a_w equal to 1.0, 0.931 and 0.872, respectively, for LEO and 1.0, 0.901 and 0.862 for PP. Shaded area corresponds to $\Delta a_{w, \text{het}} \pm 0.025$. Markers correspond to experimental measurements reported by Rigg et al. (2013); error bars represent an order of magnitude deviation from the reported value. Bottom panels: J_{het} calculated for constant $\zeta = 0.955$ for LEO and $\zeta = 0.951$ for PP. The shaded area corresponds to $a_w \pm 0.01$ and $\zeta \pm 0.001$.